UNDERWATER MEASUREMENTS OF HEART RATE

A Thesis
Presented to
The Academic Faculty

By

Hibisca Liaw

In Partial Fulfillment
Of the Requirements for the Degree
Master of Science in Mechanical Engineering

Georgia Institute of Technology

May 2013

UNDERWATER MEASUREMENTS OF HEART RATE

Approved by:

Dr. Peter H. Rogers, Advisor
School of Mechanical Engineering
Georgia Institute of Technology

Michael Gray
School of Mechanical Engineering
Georgia Institute of Technology

Dr. Mardi C. Hastings
School of Mechanical Engineering
Georgia Institute of Technology

Date Approved: January 11, 2013

To Him whose power is made perfect in weakness

ACKNOWLEDGEMENTS

I would like to thank my advisor, Dr. Peter Rogers, for the opportunity to work on this project and for his guidance throughout the process. I would also like to thank Mike Gray and Jim Martin for their help with countless questions regarding instrumentation, materials, coding, etc. Lastly, special thanks to friends and family who walked with me and encouraged me from the beginning to the completion of this paper, with whom the journey was possible.

TABLE OF CONTENTS

LIST OF TABLES

LIST OF FIGURES

LIST OF SYMBOLS AND ABBREVIATIONS

SNR	Signal-to-noise ratio
PVDF	Polyvinylidene fluoride

SUMMARY

The objective of this project is to develop a device that can monitor the heart rate and respiration of cetaceans. This would provide a way to quantitatively measure stress and determine the impact of human activity on cetaceans, especially for certain species that have been difficult to monitor in the past. There are many challenges to developing such a device, including determining the appropriate type of sensor, reducing the effect of flow noise, and designing an effective attachment method; this paper primarily focuses on determining the most suitable acoustic transducer. Experiments were conducted to compare various acoustic sensors in detecting heart rate. The electronic stethoscope performed the best in the experiments, but the results showed that other transducers, such as accelerometers and pressure sensors, also performed well and could be successful options with further development. Data processing methods to identify heartbeats and characterize signals are also discussed in this paper. Future work on the project involves subsequent tests to address other design variables as well as replicate experiments on animals.

CHAPTER 1

INTRODUCTION

1.1 Motivation

Cases of cetacean strandings (i.e. primarily whales and dolphins stranded onshore) within the past few decades have brought attention to the increased need to further study the effects of human activity on marine life. There is a particular interest in monitoring the responses of beaked whales to sonar activity, as the incidents suggest a correlation between the presence of sonar signals and beachings of various beaked whales (Cox, Ragen et al. 2006). Unfortunately, not much is known about beaked whales, because they have always been very difficult to observe. Only recently have researchers found that beaked whales are among the deepest divers in the ocean, reaching depths around 1 km (Johnson and Tyack 2003; Madsen, Johnson et al. 2005; Tyack, Johnson et al. 2006). Research in the impact of anthropogenic sound on marine animals has also been limited, but experiments such as those conducted by Nowacek, Johnson et al. (2004) show that it is possible to measure behavioral responses to human activity quantitatively.

Cox, Ragen et al. (2006) presented a comprehensive review of recent beaked whales strandings, the current understanding of the impact of anthropogenic sound on beaked whales, and recommendations for areas of research. Events where multiple strandings coincided with sonar activity include, but are not limited to: 12 Cuvier's beaked whales stranded in Greece in 1996, 17 cetacean beachings in the Bahamas in 2000, and 14 beaked whales stranded in the Canary Islands in 2002. Although a cause and effect relationship has not been definitively proven, there are a few possible

explanations for how sonar could result in strandings. Loud sound sources at certain frequencies could cause behavioral change, physiological change, or tissue damage, leading to stranding and sometimes death. There is a great need to develop technology and design experiments to investigate these possibilities.

1.2 Objective

The objective of this project is to address the previously mentioned need by developing a non-invasive device that can monitor the heart rate and respiration of free-swimming cetaceans. This would not only aid in obtaining behavioral and physiological information of the animals in their natural environment, but it would also provide one method for researchers to quantitatively measure the effects of human activity. The use of heart rate as a reflection of stress is supported by distinct correlations between human behavioral responses to stimuli (startle, defensive, and orienting responses) and changes in heart rate, first presented by Graham (1979). Heart rate also has been used in subsequent studies to monitor the response of terrestrial mammals to stimuli (MacArthur, Johnston et al. 1979; Berntson and Boysen 1984). Although heart rate data has not yet been used in similar studies for marine animals, respiration data has been shown to reflect the presence of stimuli (Spencer, Gornall et al. 1967).

There are many challenges to designing a successful device, as outlined in the next section, but this paper focuses on determining the most appropriate acoustic transducer to detect heart rate underwater. Many measurements of heart rates have been collected for marine animals through electrical means, i.e. electrocardiograms, as presented later in a review of the literature. However, the development of EKG analysis and application to free-swimming, deep-diving species has been limited due to the

difficulty in accessing attachment locations. This project will attempt to collect heart rate measurements by acoustical means, as experiments such as those done by Burgess, Tyack et al. (1998) have shown to be promising. Active sensors would require significantly more power (i.e. large batteries) than passive sensors, which would add considerable mass to the tag. Additionally, given that active acoustic sensors may have adverse effects on marine life, passive acoustic sensors such as stethoscopes, accelerometers, and hydrophones will be examined to determine the most suitable method. Due to the limitations on working directly with whales, the preliminary analysis of sensors will be done through experiments with humans. The focus was on measuring heart rate, and measurement of respiration was not studied in the experiments.

The hypothesis for this project is that an accelerometer would perform the best in obtaining heartbeat signals. Human heart sound generation can be modeled as an acoustic dipole (Kasoev 2005), and the kinetic energy is much greater than the potential energy in the near-field ($r << \lambda$, where r is distance and λ is wavelength) of a dipole (Pierce 1989). Therefore, an accelerometer, whose output is related to kinetic energy, would be a better transducer than a pressure sensor, whose output is related to potential energy.

1.3 Design challenges

Some of the design challenges for developing this device are presented below. Other issues not discussed in detail include attachment, weight and size limits, recording methods, and the means to power the device.

1.3.1 Transducer

Determining the appropriate transducer for detecting heart rate underwater requires addressing a number of issues. The first is working with the anatomy of the

whale itself. The sensor location is generally limited to the dorsal side when tagging free-swimming whales; thus, the sensor is farther away from the heart (than if it were mounted on the ventral side), and the lungs create an additional obstacle between the heart and the sensor. Fortunately, as cetaceans dive to great depths, their lungs collapse (e.g. *Tursiops truncatus* has an estimated lung collapse depth of 70 m) and thus become less of a concern (Ridgway and Howard 1979). There is also the challenge of a large range of beaked whale sizes, from about 4 m to more than 12 m in length (Organisation Cetacea), which means there will also be a large range of distances between the heart and the sensor.

The second issue is dealing with the underwater environment. The response and effectiveness of the transducers normally used in air need to be studied for applications in the water. For example, although stethoscopes have undergone extensive development in order to clearly hear heart sounds, they have not been used in the underwater context, and their optimality for such use is debatable. Another aspect of the underwater environment is the hydrostatic pressure at great depths. The ideal transducer must not only be able to survive extreme pressures but must also function correctly at depth.

1.3.2 Flow noise

One of the biggest hurdles at the present time is the issue of flow noise, i.e. the noise generated by flow over the surface of the animal. High levels of flow noise could mask the desired signal and prevent meaningful data from being collected. Although a small sample of heart rate data has been collected during dives for a few species across various experiments, the portion of decipherable data has only occurred in the absence of

flow noise, when the animal was at rest at the surface or at rest underwater (Fletcher, Le Boeuf et al. 1996; Burgess, Tyack et al. 1998; Johnson 2001; Miksis, Grund et al. 2001).

The primary issues in overcoming flow noise are in the tag geometry. One aspect involves designing the orientation and housing of the sensor so that no extra turbulence is created by the presence of the sensor and minimal flow is detected by the sensor. Additionally, techniques to reduce flow noise by separating the sensor from the fluid flow and optimizing the number and geometry of sensors, as suggested by Ko and Schloemer (1992), should be investigated.

Secondary approaches to addressing flow noise involve data processing. In the event that the recorded signal is masked or distorted by flow noise, analog or digital filtering methods may be able to extract heart rates. A robust data processing solution needs to be developed to handle a range of flow noise levels.

CHAPTER 2

BACKGROUND

2.1 Literature Review: Past experiments

From a review of the literature, it appears that there have been no successful measurements of heart rate on free-swimming cetaceans to date. Experimental results have included heart rate data for captive whales and other marine animals, but experiments containing heart rate data for free-swimming animals have been few. One experiment conducted by Burgess, Tyack et al. (1998) recorded heart beats on tagged elephant seals, but the signals were identifiable only in the absence of flow noise. A recent experiment with free-swimming beaked whales (Tyack, Johnson et al. 2006) collected dive profile information and recorded animal vocalizations and ambient noise but did not attempt to detect heart rate.

2.1.1 Heart rates of whales

Studies measuring heart rate of whales have been conducted beginning in the mid-1900s. King, Jenks Jr et al. (1953) were able to record an electrocardiogram (EKG) of a male beluga whale (*Delphinapterus leucas*) by using a harpoon as a lead. The heart rate ranged from 12 to 24 bpm, and they concluded that the EKG had similar characteristics to that of other mammals. Much later, Meijler, Wittkampf et al. (1992) also recorded an electrocardiogram, using a suction electrode to measure the heart beats of two humpback whales (*Megaptera novaeangliae*) trapped in nets. Ponganis and Kooyman (1999) measured similar data on a captive gray whale (*Eschrichtius robustus*) in 1999 also by

attaching electrodes while it was inactive. They found the resting heart rates to be 24-35 bpm.

2.1.2 Heart rates of other cetaceans

The heart rates of other cetaceans, mostly dolphins, have also been measured in the past. Elsner, Kenney et al. (1966) studied the effect of diving on the heart rate of bottlenose dolphins (*Tursiops truncatus*) and found that there was sudden bradycardia that occurred during dives. In the study, the heart rate data was collected by attaching electrodes to a rubber belt that the dolphin wore. Williams, Friedl et al. (1993) studied the effect of exercise on heart rate of bottlenose dolphins. Later in 1999, Williams followed up with more reports on the effects of exercise and diving on heart rate in bottlenose dolphins (Williams, Haun et al. 1999; Williams, Noren et al. 1999). Because all the dolphins in the experiments were trained, they were able to attach the sensors using a combination of suction cups and a nylon harness.

Instead of using electrodes, Miksis, Grund et al. (2001) used a hydrophone potted in a suction cup to measure heart rate, and heart beats were recorded while the trained dolphins remained still, creating a situation of no flow. An average heart beat profile was determined and used in a matched filter to calculate a heart rate. Heart rates were found to be 23-46 bpm, with a spectral range of 10-200 Hz. Figure 2.1 shows hydrophone signals of baseline heartbeats for two dolphins. The suction cup containing the hydrophone was placed along the ventral midline.

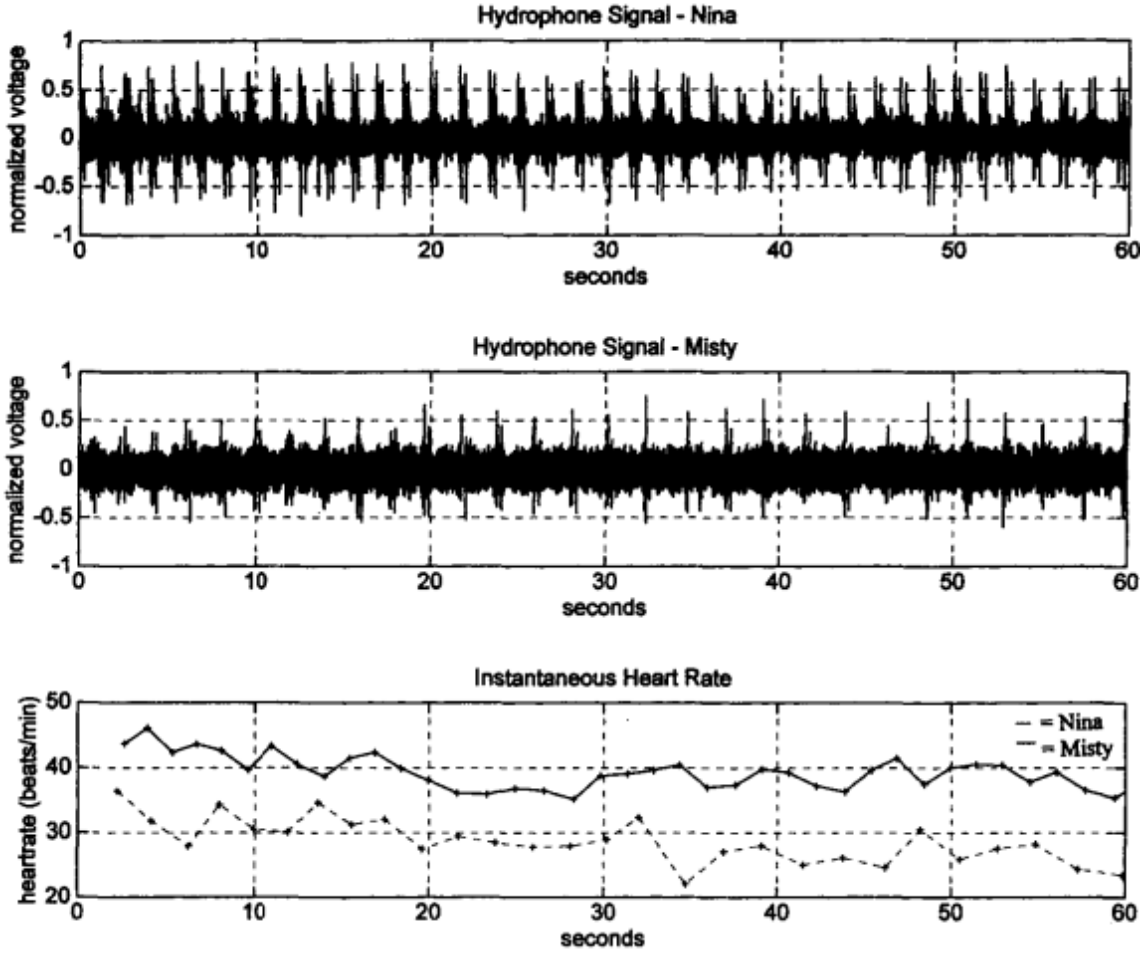

Figure 2.1: Hydrophone signals of dolphin heartbeats (Miksis, Grund et al. 2001).

In addition to dolphins, the heart rate of killer whales (*Orcinus orca*) has also been studied. Spencer, Gornall et al. (1967) observed patterns breathing of killer whales and studied heart rate in EKG data by attaching electrodes to one killer whale during transport and one beached whale. They found the heart rates alternating between 30 and 60 bpm, and noted that the variation in heart rate depending on respiration was comparable to that observed in humans.

2.1.3 Underwater heart rates of other animals

The heart rates of other animals, underwater, have also been studied. Wolf (1965) presented his observations on the human dive reflex from experiments conducted on family members. The dive reflex was triggered by immersing the face in water. Immediate bradycardia was observed with face immersion, whereas bradycardia occurred later with normal breath holding. Additionally, Wolf found that mere anticipation of face immersion also prompted immediate bradycardia.

The heart rates of other animals have also been studied. Elsner (1966) observed the heart rate of a hippopotamus at a zoo by cementing electrodes on its back. They observed that even during dives shorter than one minute that there was similar bradycardia to that observed in other marine animals. Claireaux, Webber et al. (1995) observed the physiological and behavioral responses of captive Atlantic cod (*Gadus morhua*) to temperature changes. Heart rates were monitored using surgically implanted electrodes for an EKG transmitter.

Fletcher, Le Boeuf et al. (1996) recorded heart and respiration sounds from hydrophones attached to elephant seals (*Mirounga angustirostris*). They glued neoprene patches and attached the instrumentation onto the seals while they were immobilized and then released them back into the ocean. Although the goal of the study was to record external noises during the seals' dives, they found clear heart rates and breathing patterns from recordings while the seals were at the surface of the water, as shown in Figure 2.2.

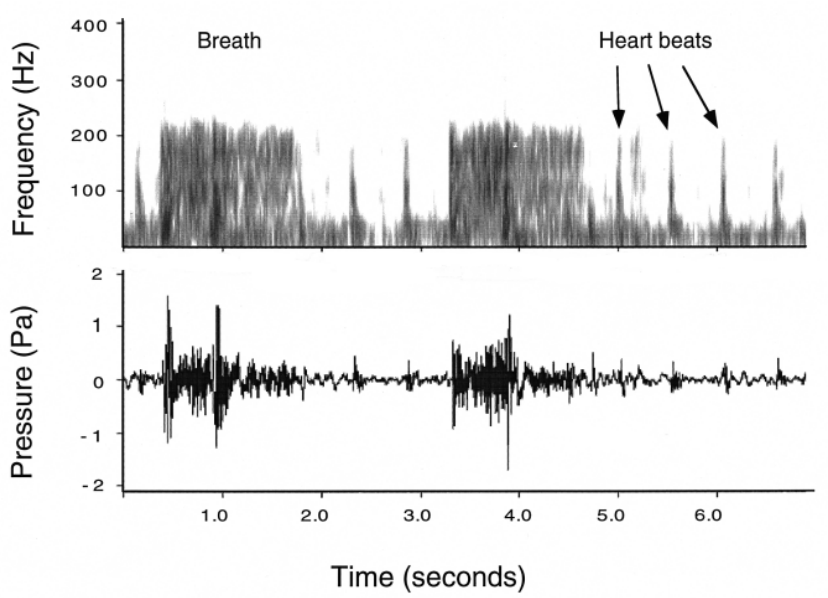

Figure 2.2: Spectrogram and waveform of elephant seal respiration and heartbeats at the surface between dives (Fletcher, Le Boeuf et al. 1996).

Burgess, Tyack et al. (1998) also reported data from an acoustic recording tag that was developed and used on elephant seals. They noted that the peak flow noise was around 10 Hz, which is in the same range as heart beat sounds. Although the filtering processes were unable to extract a heart rate from data collected in the presence of flow noise, heart rates were measureable when the seals were at rest at the surface and when they were at rest at depth. They also observed bradycardia, with heart rates of 120 bpm at the surface, 60 bpm underwater in the surface interval, and 42 bpm at the bottom of a dive, as shown in Figure 2.3.

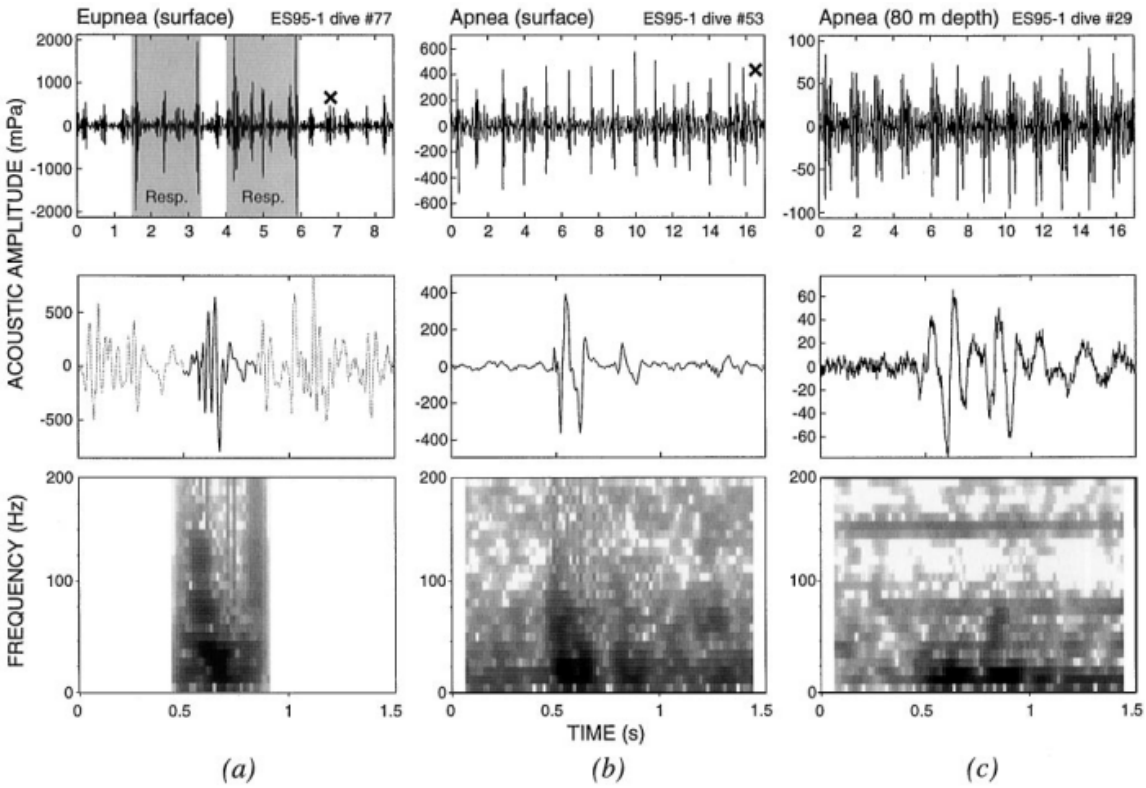

Figure 2.3: Respiration and heartbeats recorded from elephant seals.
Top row shows acoustic waveforms with a low-pass filter of 40 Hz; middle row shows superposed cardiac signature with a low-pass filter of 300 Hz; bottom row shows phonocardiograms (Burgess, Tyack et al. 1998).

More recently, Meir, Stockard et al. (2008) monitored the heart rates in diving emperor penguins (*Aptenodytes forsteri*) by implanting electrodes. They observed extreme bradycardia, recording heart rates ranging from 256 bpm in the surface interval to 6 bpm at depths, compared to resting heart rates of 63-84 bpm.

CHAPTER 3

METHODS

In order to design a device that can monitor the heart rate of whales, an appropriate sensor must first be established. Thus, it was important to compare potential transducers in a variety of experimental settings to determine a robust transducer for the task. Due to the nature of the experiments, it was easier to first conduct experiments with humans before pursuing experiments with whales. Two sensors experiments are presented below.

3.1 Sensor Comparison Experiment, v.1

The first sensor comparison experiment was comprised of four parts. The first and main objective was to compare previously existing sensors under different circumstances. The second and third parts characterized two noise conditions present in the main experiment, and the last part developed a data processing method.

3.1.1 Sensor Comparison

3.1.1.1 Objective

The objective of this part of the experiment was to compare the signals from different sensors detecting human heart rate in air, still water, and flowing water. The sensors being tested were: an acoustic stethoscope, an electronic stethoscope, an accelerometer, a hydrophone, and a customized sensor package containing one accelerometer and one hydrophone. Heartbeat measurements were taken from both the

ventral and dorsal sides, and recordings were taken for different breathing patterns to simulate various lung inflation conditions.

3.1.1.2 Apparatus

The apparatus used in the procedure included the sensors: an acoustic stethoscope, an electronic stethoscope (Welch Allyn Master Elite 5079-405), a single-axis accelerometer (Edo 5185-2), a hydrophone (Brüel & Kjær 8103), and a customized sensor package containing one single-axis accelerometer (Edo 5185-2) and one hydrophone (International Transducer Corporation 6166) potted in a polyurethane elastomer (BJB ST-1085). The sensors are shown below in Figure 3.1 and Figure 3.2.

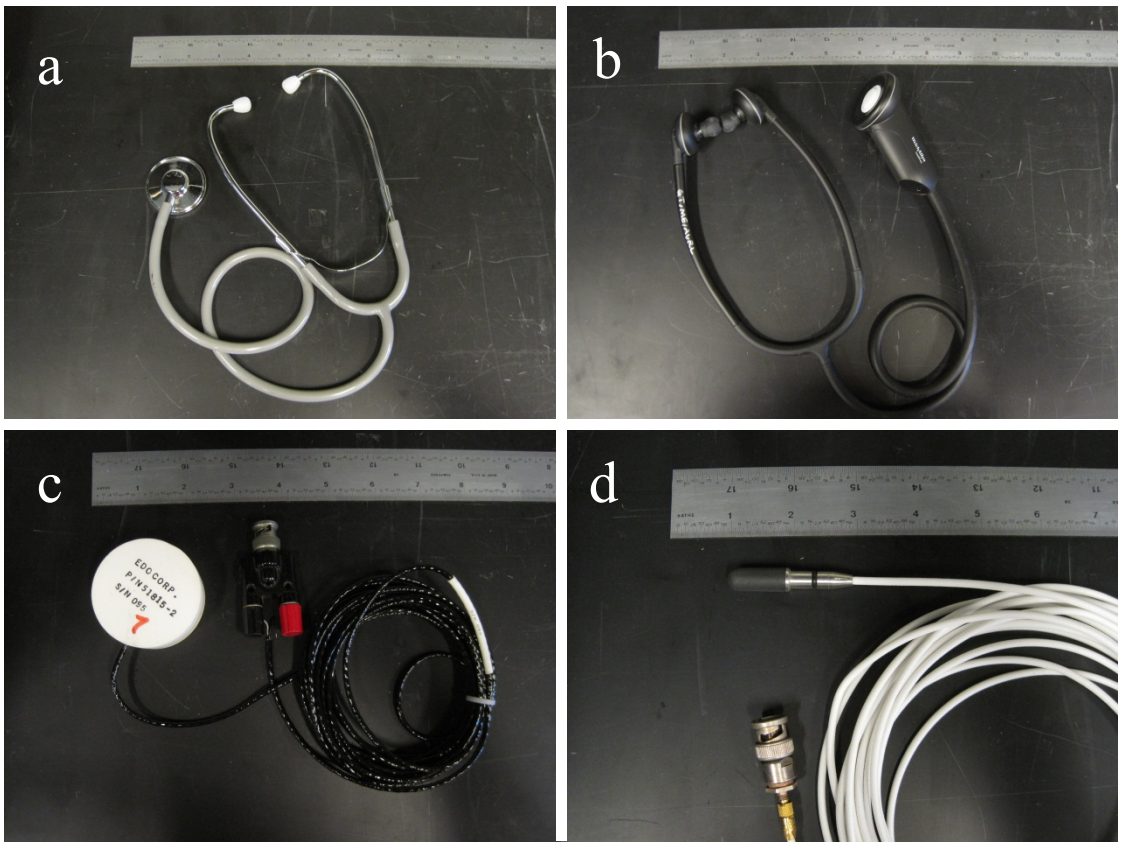

Figure 3.1: Sensors used in the first sensor comparison experiment.
(a) acoustic stethoscope, (b) electronic stethoscope, (c) accelerometer, (d) hydrophone.

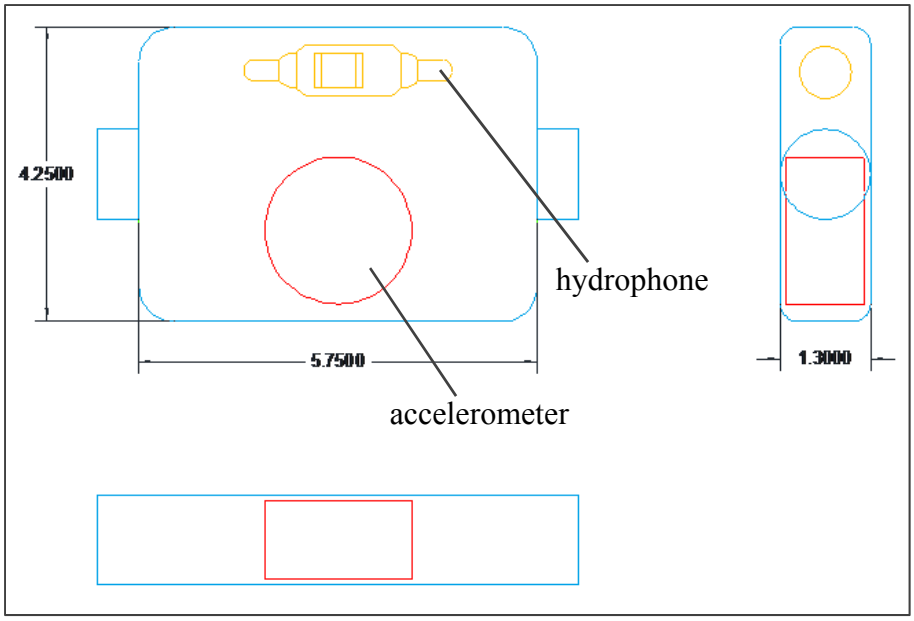

Figure 3.2: Sensor package used in the first sensor comparison experiment.

The physical setup of the apparatus is shown below in Figure 3.3. The electronic stethoscope was directly connected to a portable digital recorder (Zoom H2). The accelerometers and hydrophones were connected to a pre-amplifier (Stanford Research SR560) before connecting to the recorder. Other apparatus included an adjustable stool about 18” tall and a food storage bag to protect the stethoscopes in water. The full measurement configuration is shown below in Figure 3.4.

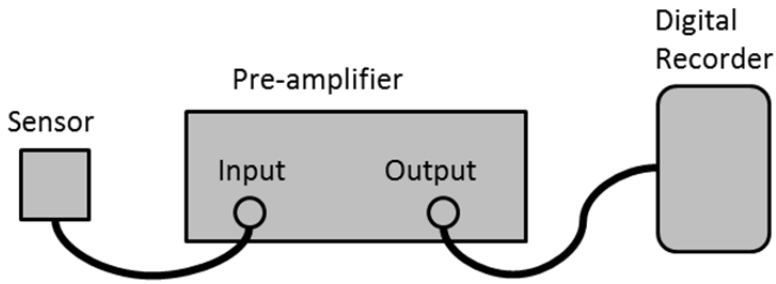

Figure 3.3: Apparatus setup for the sensor comparison experiment.

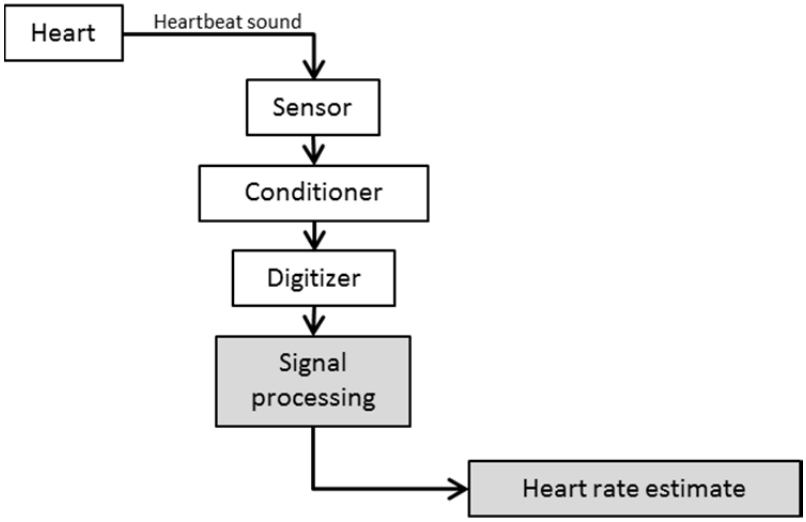

Figure 3.4: Measurement configuration for the sensor comparison experiment. Signal processing and heart rate estimate were performed post- data collection.

3.1.1.3 Procedure

3.1.1.3.1 Set-up

The experiment was conducted at the Georgia Institute of Technology Campus Recreation Center in the Lazy River section of the Crawford pool. The pool was closed to the public at that time to minimize background noise. Lifeguards were present throughout the duration of the experiment. There was also an assistant to help collect data.

The participants were male volunteers in the age range of 18-25. All volunteers were required to complete a swim questionnaire to ensure they knew how to swim. Although electrical components of the sensors were used in water, all electronics were battery-powered. All testing involved in the experiment was non-invasive and should not have caused even minor discomfort to the volunteers. The procedures were approved by the Georgia Institute of Technology Institutional Review Board.

3.1.1.3.2 Sensor Comparison Experiment

Each volunteer first changed into a swimsuit and then sat on the provided stool out of the water. The location for detecting heartbeats was marked with a permanent marker on both the ventral and dorsal sides. For both, the location was the third intercostal space on the left side called Erb's point, which is one of the traditional auscultatory areas, as shown below in Figure 3.5 (Lippincott 2009). Only one location was chosen in order to avoid prolonged experiment times for each volunteer.

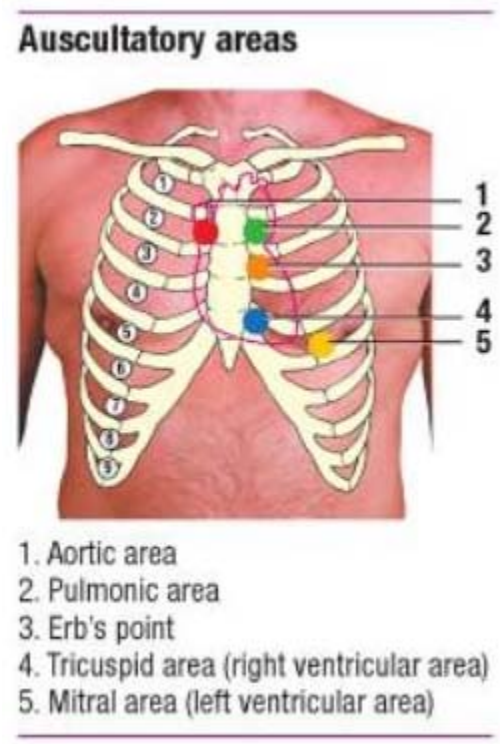

Figure 3.5: Traditional auscultatory areas (Lippincott 2009).

The researcher held the acoustic stethoscope on the marked location and recorded qualitative observations. The researcher then held the electronic stethoscope on the marked location and the assistant recorded the heartbeat for 10 seconds with the volunteer breathing normally. A second recording of 10 seconds was taken with the

volunteer holding his breath after inhaling. A third recording of 10 seconds was taken with the volunteer holding his breath after exhaling. Three trials, each with three recordings, were conducted for both the ventral and dorsal sides. Similarly, data was collected using the accelerometer, the hydrophone, and the sensor package. The sensor package was aligned so that the two sensors were on the same level horizontally and the midpoint between the two sensors was positioned over the marked location.

The procedure was repeated with the volunteer sitting on the stool in still water. The stool was adjusted so that the torso was completely submerged, but the water did not rise above chin-level, as shown in Figure 3.6.

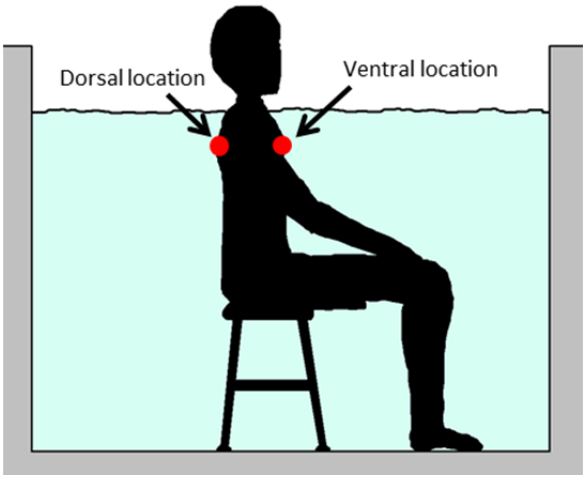

Figure 3.6: Side view of volunteer in the Lazy River, showing water level and measurement locations.

Lastly, the pumps in the Lazy River were turned on to introduce a flow. The volunteer was positioned in the center of the channel, facing one of the walls; the flow traveled from the right side of the body to the left side. The procedure for collecting data was repeated for this water flow setup.

3.1.2 Background Noise

The objective of this part of the experiment was to characterize the background noise of the first part of the experiment by determining the spectral density. The accelerometer and the customized sensor package used in the first part of the experiment were used to record the noise. Six recordings of 20 seconds each were taken; both sensors recorded ambient noise in air, still water, and flowing water. All measurements were taken with the sensor positioned in the same location and orientation as in the first part of the experiment.

3.1.3 Flow Rate

The objective of the third part of the experiment was to approximate the flow rate in the Lazy River channel. Two methods were used: the first with a current measurer called the Aquadopp, and the second with a simple setup using a stopwatch and floating object.

3.1.3.1 Aquadopp

The apparatus used in this experiment included the Aquadopp (Nortek model 6000m), the frame to hold the Aquadopp, 2x4 wood boards to suspend the frame in the flow channel, and a laptop to record data. The Aquadopp was positioned in the middle of the Lazy River where the measurements from the first part of the experiment were taken, as shown in Figure 3.7. The measuring location was about 3 inches below the surface, approximately where the sensors were placed on the volunteers' as they sat in the water. The Lazy River was turned on to create a current.

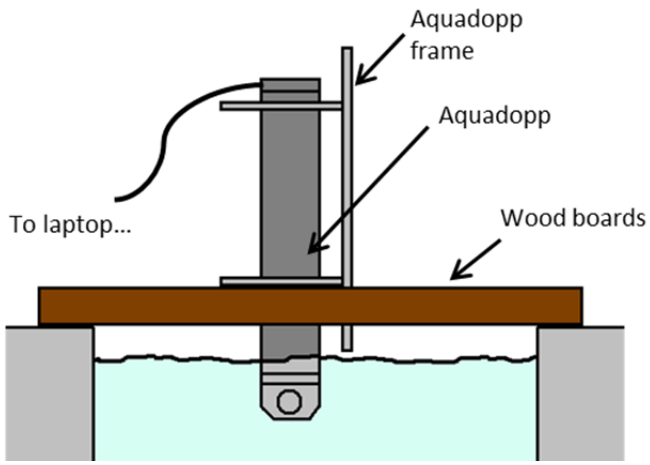

Figure 3.7: Side view of Aquadopp setup; flow direction is into the page.

Four sets of data of about 50 seconds were recorded; two sets were taken with a measurement interval (i.e. time between each measurement) of 2 seconds and an average interval (i.e. period during the measurement interval of active measurements) of 1 second, and two sets were taken with a measurement interval of 5 seconds and an average interval of 2 seconds. All measurements were taken with a blanking distance of 0.35 m.

3.1.3.2 Floating object

The apparatus used in this part of the experiment included a fishing float with weights attached, a tape measure, and a stopwatch. Measurements were taken in a 1.83-m (6-ft) section of the Lazy River where the measurements from the first part of the experiment were taken. The Lazy River was turned on to create a current.

The measurement section was marked on the pool deck next to the channel with the tape measurer. The fishing float was released upstream of the measurement section in the middle of the channel; the trajectory in the measurement section was then timed and recorded. Fifteen trials were recorded, fourteen with the fishing float and one with an orange peel that was contained in the current.

3.1.4 Data Processing

It was important to develop a method of data processing that would be sufficiently robust to handle all of the data collected from the sensor comparison experiments. The method needed to be able to process a raw recording and quantify both the heart rate and the signal-to-noise ratio (SNR). All recordings were sampled at 44.1 kHz and recorded at 16 bits.

3.1.4.1 Improve SNR

The most difficult part of the data processing involved improving the SNR to better extract the heart rate from the filtered sample. This process was performed on all recordings, including those that already contained clear heartbeats. Three methods are discussed below.

3.1.4.1.1 Average Signal

The first approach was to create an average heart beat signal that would represent the ideal heart beat waveform. It could then be used to cross-correlate with a full recording to improve its SNR. This method was successful in reports by Burgess, Tyack et al. (1998) .

The original recording was filtered to remove outliers and a 200-Hz low-pass filter was applied. To create an average signal, recorded signals with a clear “lub-dub” heart beat were averaged together. The “lub” and “dub” sounds, i.e. the first and second heart sounds (S_1 and S_2), are caused by certain heart valves closing at those two moments (Ronan Jr 1992). Various windows (i.e. “lub-dub”, “lub-dub + noise”, “lub”, etc.) were tested to find one that improved the SNR the most. An average signal was created for the electronic stethoscope using “lub-dub + noise” windows from seven clear heart beats

within a recording, shown below in Figure 3.8. Similar average signals were also created for the accelerometer and the hydrophone.

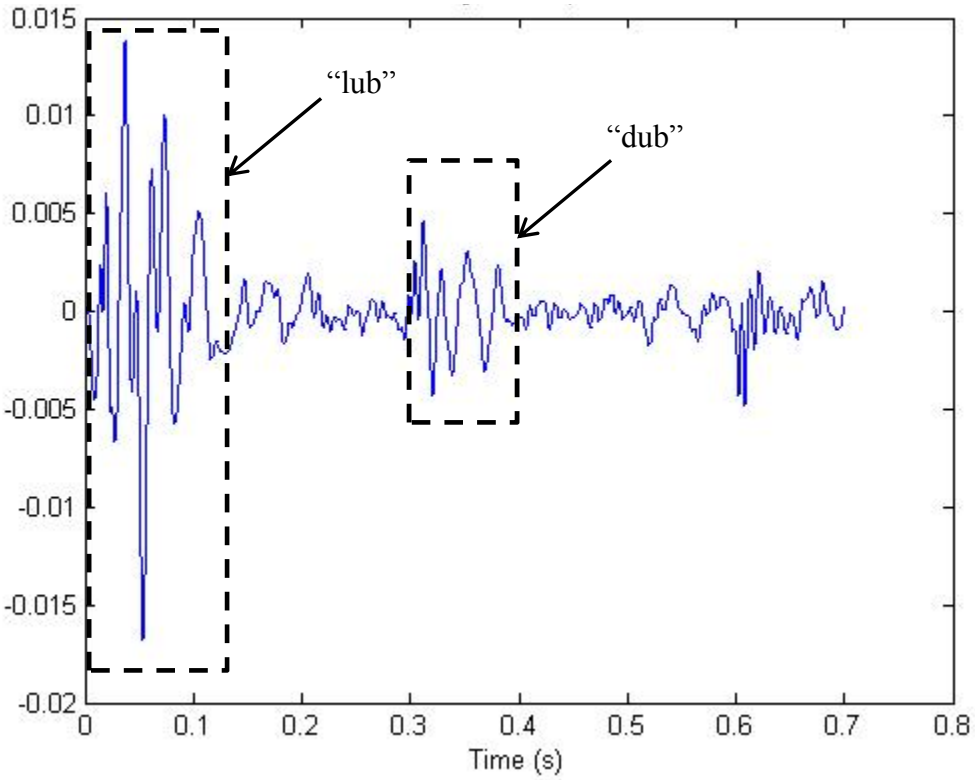

Figure 3.8: Average signal for the electronic stethoscope.

3.1.4.1.2 Autocorrelation

The second method was to cross-correlate each recording with itself. This method creates a maximum peak at the middle of the correlation with side lobes decreasing in amplitude. The spacing of the side lobes correspond to the heart rate in the signal. The original recordings were first filtered to remove outliers and a 100-Hz low-pass filter was applied before cross-correlation. An example of autocorrelation with an ideal periodic signal is shown in Figure 3.9.

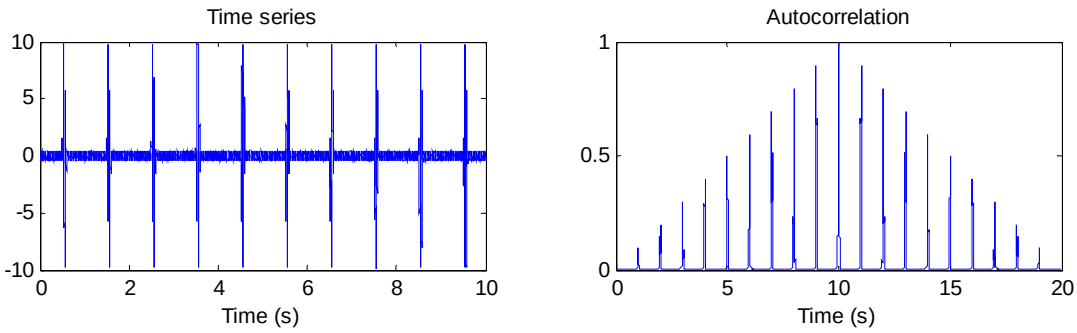

Figure 3.9: Autocorrelation for an ideal periodic signal.

3.1.4.1.3 Spectrogram

The third method was to create a spectrogram (spectral density vs. time) for each recording using a sliding fixed width time window. Fletcher, Le Boeuf et al. (1996) reported observing clear heart beats and respiration indicators using this method, suggesting it was a viable method. Assuming that heart beat sounds and noise have different frequency contents, the spectrogram would help distinguish between signal and noise. The MATLAB spectrogram function was tested on a few recordings from various sensors. An example spectrogram of an ideal periodic signal is shown in Figure 3.10.

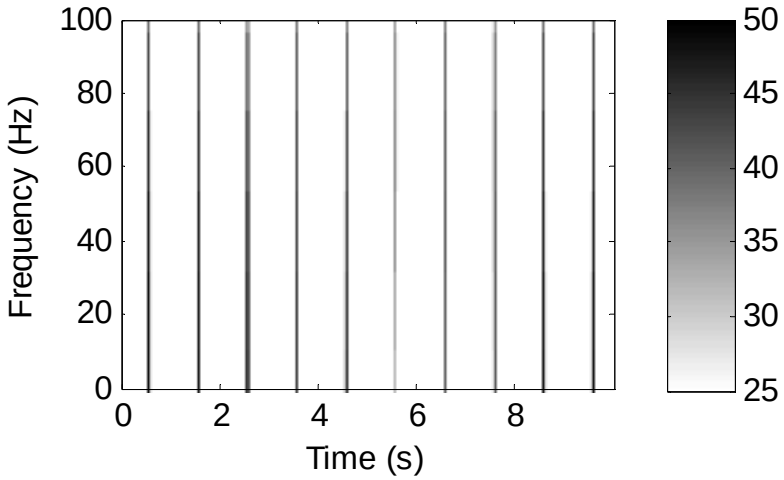

Figure 3.10: Spectrogram for an ideal periodic signal.

3.1.4.2 Determine Heart Rate

Once the SNR was improved so that heart beats were visible in the signal, it was necessary to develop a method to identify heart beats and return a heart rate. This could be accomplished manually, using visual and audial cues to find the heart beat peaks for each recording, but the ideal solution would return a heart rate by supplying only the raw recording.

An automated method was developed for a signal that was first processed with autocorrelation. The result from autocorrelation would reveal any periodic signals in the recording, which would be determined as heartbeats if the heart rate was assumed to be constant. The heart rate for a given recording would be calculated from the time difference between the maximum peak at the middle and the first side lobe, which are shown in Figure 3.11. To identify the first side lobe, an expected heart rate range was used to determine a side lobe window, as shown in Figure 3.12. The calculated center of mass for the side lobe window was designated as the first side lobe location. The expected heart rate range was set to 55-100 bpm, and the side lobe window was 0.113 seconds (5000 samples at a sampling rate of 44.1 kHz).

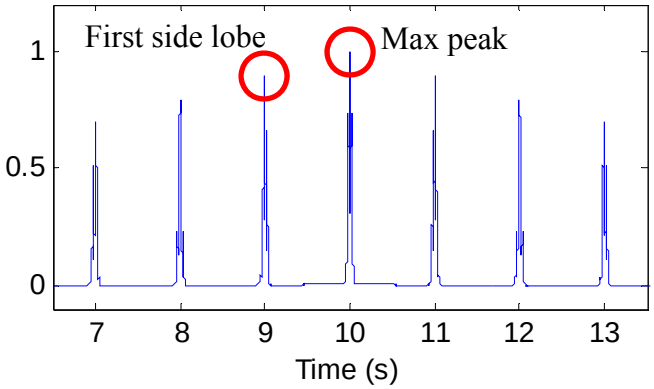

Figure 3.11: Close-up of autocorrelated signal, showing max peak and first side lobe.

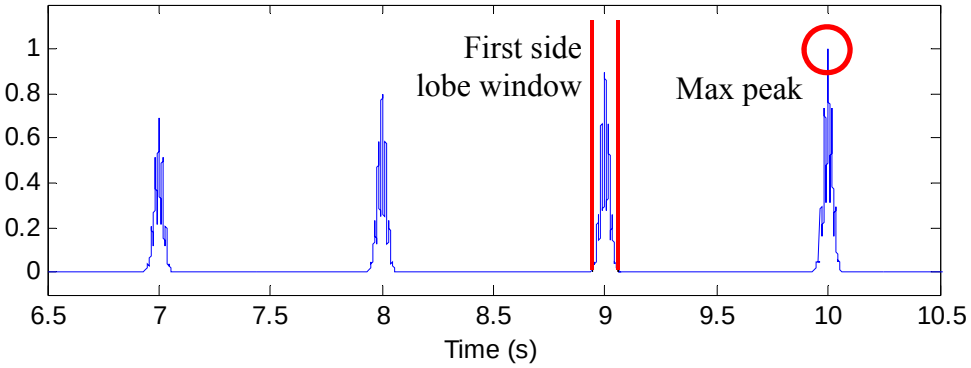

Figure 3.12: Close-up of autocorrelated signal, showing the first side lobe window.

3.1.4.3 Determine SNR

The last value to quantify is the SNR of the final, processed signal. The SNR (in dB) is defined as shown in Eq. (3.1)

$$\mathrm{SNR} = 20\log\left(\frac{A_{\mathrm{signal}}}{A_{\mathrm{noise}}}\right) \tag{3.1}$$

where A_{signal} is the root-mean-square (RMS) signal level and A_{noise} is the RMS noise level. The RMS signal level was calculated using the first side lobe window, and the RMS noise level was calculated using the window between the first and second side lobes.

3.2 Sensor Comparison Experiment, v.2

The second sensors experiment was conducted at a much later time (after the analysis of the first sensors experiment), and it was comprised of three parts. The first part was to design new transducers to be used in the subsequent sensor comparison experiment. The second part was to compare the new transducers with previously existing sensors, using the same method as in the first sensor comparison experiment. Lastly, the third part was to develop an improved data processing method.

3.2.1 Sensor Design

The goal of designing new sensors was to create housed sensors in order to have a more equal comparison with previously existing, housed sensors. The housing was expected to reduce the amount of noise in the recordings. Two sensors were created in preparation for the sensor comparison experiment: an accelerometer sensor and a pressure sensor. The accelerometer sensor was composed of an accelerometer surrounded by foam. The pressure sensor was modeled from an electronic stethoscope transducer and composed of a strip of piezoelectric foil wrapped around a cylindrical, rubber core. Each transducer was encased in a cylindrical housing that was rigid on all sides except for one end covered by a flexible membrane.

3.2.1.1 Accelerometer Sensor Design

The accelerometer sensor layout is shown below in Figure 3.13. A Vibra-metrics miniature single-axis accelerometer, with an internal amplifier, Model 9002A, was encased in syntactic foam to form the accelerometer noted in the figure. A single wire from the accelerometer existed outside of the housing. The top surface of the sensor was applied to the measurement location, and the sensitive axis is noted in the figure. It was

necessary to choose the backing and surrounding materials and determine the dimensions that would allow for an appropriate accelerometer response. The effects of material properties and dimensions were examined through models, and results from experimental testing were compared to the models.

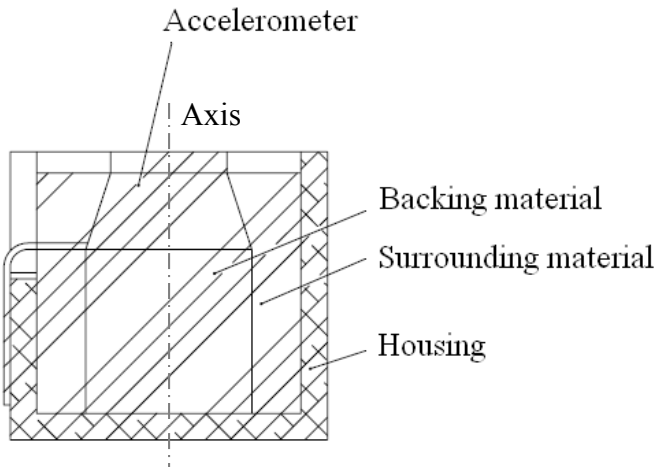

Figure 3.13: Section view of the housed accelerometer sensor.

There were a few factors to consider in choosing materials. Ideal materials would be more compliant than water but still withstand hydrostatic pressure at great depths in future experiments. Given the shallow testing depths in this experiment, hydrostatic pressure was not an issue. However, there were two resonance concerns: mass-spring resonance and standing wave resonance within the backing material.

First, a simple mass-spring model, shown in Eq. (3.2), was used to predict the response of the system, where F is the input force, m is mass, k is the spring constant, and x is position. Eq. (3.3) shows the transfer function of acceleration to input, where s is the Laplace variable, and Eq. (3.4) gives the predicted accelerometer response, $A(\omega)$, where ω is frequency in radians, $I(\omega)$ is the input drive force, and $H(\omega)$ is the system transfer function.

$$F = mx'' + kx \tag{3.2}$$

$$H(s) = \frac{A(s)}{F(s)} = \frac{s^2}{ms^2+k} \tag{3.3}$$

$$A(\omega) = I(\omega) \cdot H(\omega) \tag{3.4}$$

By modeling the accelerometer as the mass and the backing material as a spring (and ignoring the effects of the surrounding material), a Bode diagram was used to analyze the frequency response of the sensor. The goal was to obtain a low natural frequency while maintaining a flat response in the low frequency range.

The backing material was modeled as a spring, using Eq. (3.5)

$$k = \frac{EA_0}{L_0} \tag{3.5}$$

where k is the spring constant, E is the Young's modulus, A_0 is the original cross sectional area, and L_0 is the original length. A complex Young's modulus, shown in Eq. (3.6), was used in the model to account for loss. E_{exp} was found experimentally, as described in a later section, and a loss factor of 0.07 was estimated for η (Madigosky and Lee 1979).

$$E = E_{\text{exp}}(1 + \eta i) \tag{3.6}$$

The effective mass used in the model included the mass of the accelerometer, the effective spring mass,$m_{\text{eff,sp}} = \frac{1}{3} m_{\text{sp}}$, and the radiation mass. The radiation mass shown below in Eq. (3.7) was calculated using an end correction for a thin walled tube (Levine and Schwinger 1948) shown in Eq. (3.8)

$$m_{\text{rad}} = \rho \pi a^2 \Delta l \tag{3.7}$$

$$\Delta l = 0.61a \tag{3.8}$$

where m_{rad} is the radiation mass, ρ is the density of the fluid, a is the radius of the tube, and Δl is the end correction.

The second model calculated the standing wave resonance in the backing material, using Eq. (3.9) to Eq. (3.12) below

$$H_{\text{res}} = \frac{n\lambda}{2}, n = 1,2,3 \ldots \tag{3.9}$$

$$\lambda = \frac{c}{f} \tag{3.10}$$

$$c = \sqrt{\frac{K}{\rho}} \tag{3.11}$$

$$K = \frac{E}{3(1-2\nu)} \tag{3.12}$$

where H_{res} is the height of the backing material cylinder that would lead to standing resonance waves, λ is the wavelength, c is the speed of sound, f is the frequency, K is the bulk modulus, ρ is the density, E is the Young's modulus, and ν is the Poisson's ratio. Combined, H_{res} is calculated using Eq. (3.13) shown below.

$$H_{\text{res}} = \frac{n}{2f}\sqrt{\frac{E}{3\rho(1-2\nu)}}, n = 1,2,3 \ldots \tag{3.13}$$

Closed cell foam was chosen to be both the backing material and the surrounding material. Two materials, Rubatex® 451N and Monmouth Durafoam™ DK1111, were used in static testing to determine the Young's modulus of each. A long sample with a square cross-section was cut for each material, the top end was glued to a rigid surface, and the bottom end was glued to another surface on which weights were added. The added mass and the corresponding change in length of the foam sample were recorded.

After the accelerometer sensor was constructed, experimental tests were conducted to compare the results with the model. To test the frequency response, the rigid housing of the accelerometer sensor was mounted to a shaker (Labworks ET-140). The physical setup of the apparatus is shown below in Figure 3.14. The shaker was given a drive signal of a low frequency sweep (0-250 Hz) of 6 seconds long, and the

accelerometer output was recorded. The full measurement configuration is shown below in Figure 3.15. An accelerometer without housing was also tested on the shaker and compared to the housed sensor.

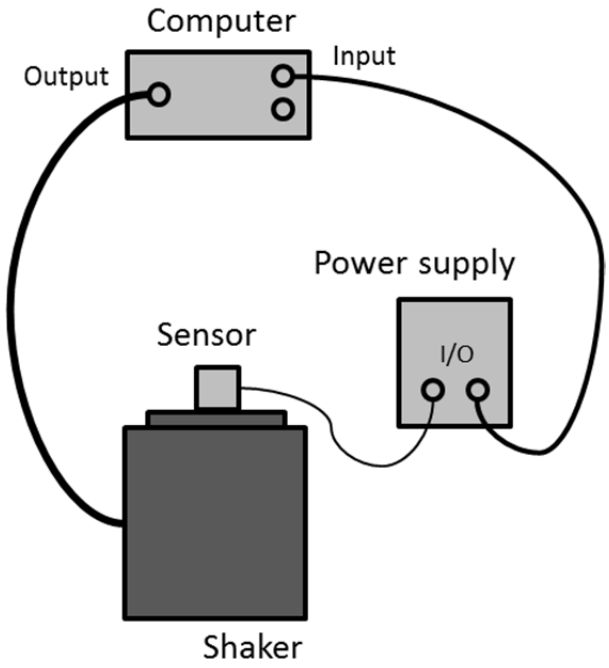

Figure 3.14: Apparatus setup for the accelerometer sensor shaker tests.

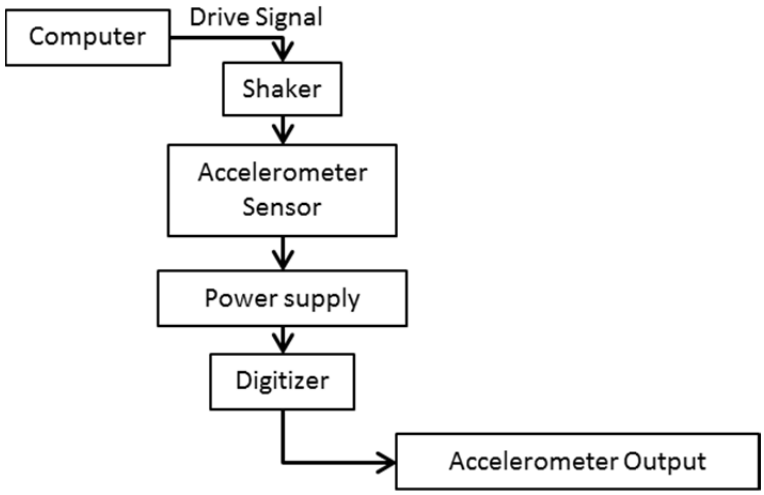

Figure 3.15: Measurement configuration for the accelerometer sensor shaker tests.

3.2.1.2 Pressure Sensor Design

The pressure sensor layout is shown below in Figure 3.16. The PVDF Sensor noted in the figure was composed of a cylindrical rubber core wrapped in a piezoelectric polymer foil, specifically polyvinylidene fluoride (PVDF). A single wire from the PVDF (not shown in the figure) existed outside of the housing. As with the accelerometer sensor, the top surface of the pressure sensor was applied to the measurement location. The PVDF responded to radial strain resulting from axial compression of the rubber core. Rubber materials and attachment methods were examined via models and experiments.

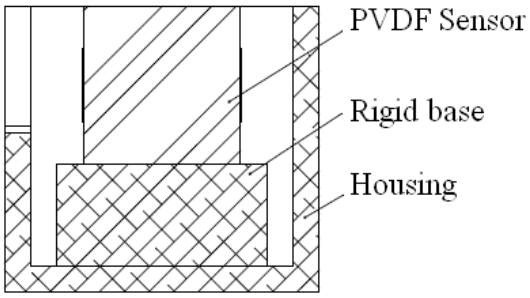

Figure 3.16: Section view of the housed pressure sensor.

A rough model of the rubber in the pressure sensor was taken from the definition of Poisson's ratio for a cylinder, shown below in Eq. (3.14)

$$\frac{\Delta d}{d} = -\nu \frac{\Delta H}{H} \tag{3.14}$$

where d is the original diameter of the cylinder, Δd is the change in the cylinder's diameter, ν is the Poisson's ratio, H is the original height of the cylinder, and ΔH is the change in the cylinder's height. To obtain the maximum sensor response (i.e. maximum Δd), the rubber would need to have both a high Poisson's ratio and high compliance (ΔH).

Two rubber materials were tested: a McMaster-Carr silicone rubber #9808K251 (3/4” diameter cord with 40A durometer) and Elastack Molding Compound. The spring constants of both rubber materials were found experimentally using an Instron machine (Model 5569). Both samples of diameter 19 mm (0.75”) and height 19 mm (0.75”) were compressed by 6 mm and the force versus compression distance data was recorded.

The two rubber materials were covered with PVDF (Images Scientific Instruments PZ-04 Raw Piezofilm Speaker Material, 52 μm thickness) using various attachment methods (i.e. single-sided Scotch tape, Loctite Black Max 380, and Loctite 290). The pressure sensors were then tested on a shaker (Labworks ET-140) against a rigid surface to create a compression situation, creating radial strain in the rubber core and output from the PVDF. The physical setup of the apparatus is shown in Figure 3.17. A laser Doppler vibrometer (LDV) (Polytec PDV-100) was mounted vertically and used to measure the response of the shaker platform. The shaker was given a drive signal of a low frequency sweep (0-250 Hz) of 6 seconds long with various attenuation settings, and the PVDF and LDV outputs were recorded. The full measurement configuration is shown below in Figure 3.18.

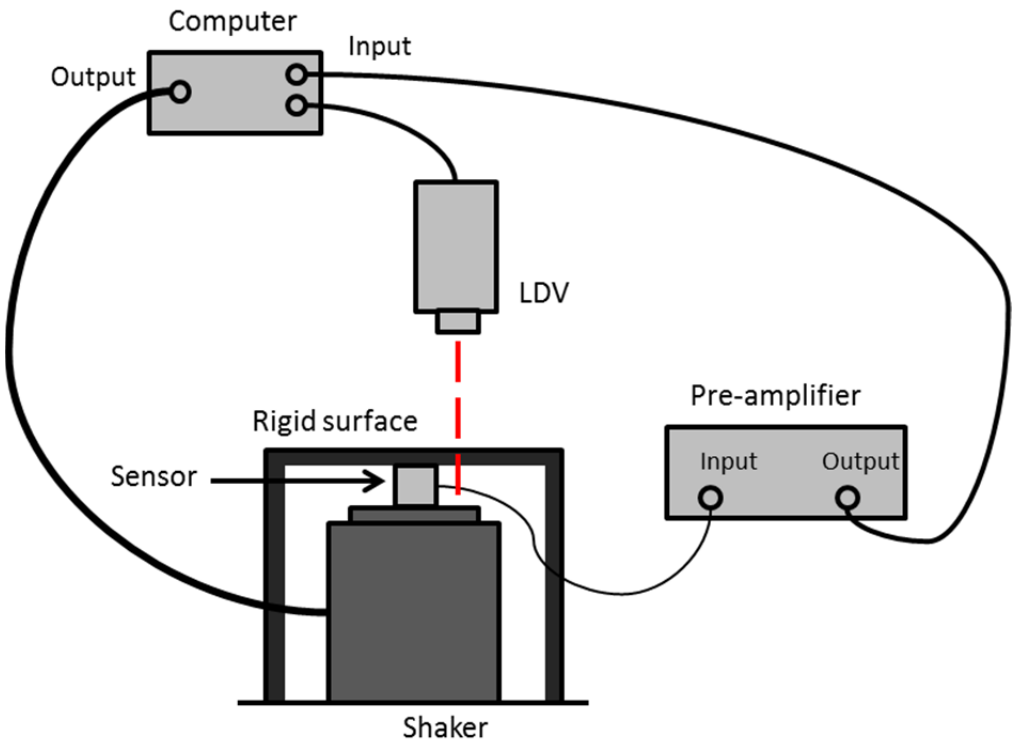

Figure 3.17: Apparatus setup for the pressure sensor shaker tests.

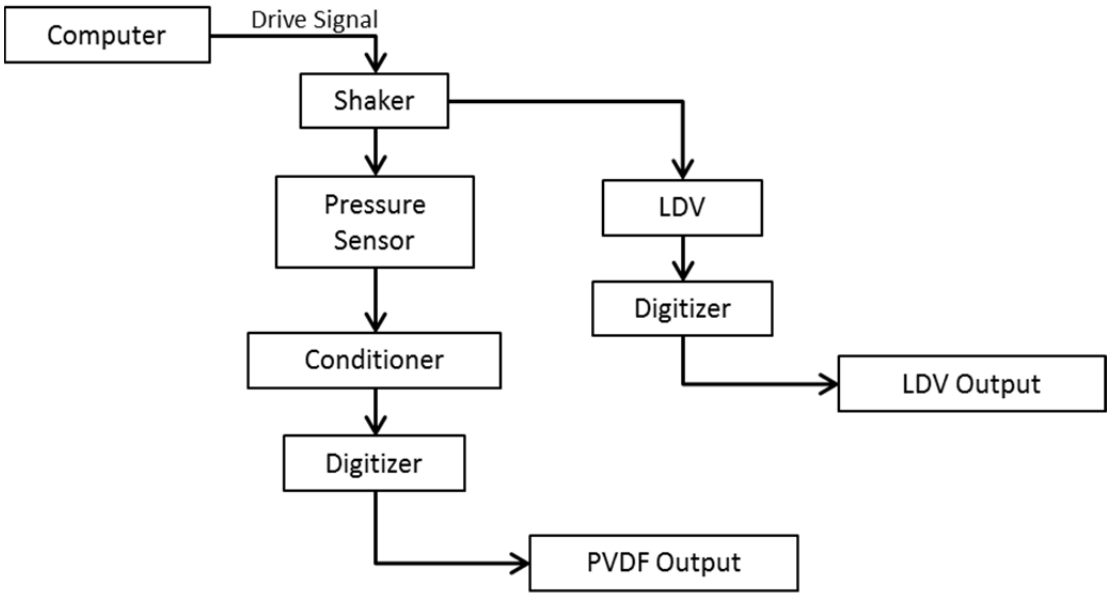

Figure 3.18: Measurement configuration for the pressure sensor shaker tests.

The PVDF output was predicted using Eq. (3.14), where the strain in the PVDF ($\Delta d/d$) would be directly proportional to the input displacement (ΔH). The response of

the shaker platform was modeled as a mass with two springs, one above (i.e. the rubber core) and one below (i.e. the shaker spring), as shown in Eq. (3.15), where F is the input force, m is the shaker platform mass, k_r is the rubber spring constant, k_s is the shaker spring constant, and x is position. The predicted resonance frequency is given in Eq. (3.16). Using the displacement transfer function given in Eq. (3.17), the modeled response was compared to the experimental results from the LDV output. Lastly, the pressure sensors were also tested with heart beat signals in air.

$$F = mx'' + (k_r + k_s)x \tag{3.15}$$

$$f_{\text{res}} = \frac{1}{2\pi}\sqrt{\frac{(k_r+k_s)}{m}} \tag{3.16}$$

$$H(s) = \frac{X(s)}{F(s)} = \frac{1}{ms^2+(k_r+k_s)} \tag{3.17}$$

3.2.2 Sensor Comparison

3.2.2.1 Objective

The objective of this part of the research was to compare the signals from different sensors detecting human heart rate in air, still water, and flowing water. The sensors being tested were: an electronic stethoscope, the customized accelerometer sensor, and the customized pressure sensor. Heartbeat measurements were taken from both the ventral and dorsal sides, and recordings were taken for different breathing patterns to simulate various lung inflation conditions.

3.2.2.2 Apparatus

The apparatus used in the procedure included three sensors: an electronic stethoscope (Welch Allyn Master Elite 5079-405), a customized accelerometer sensor, and a customized pressure sensor. The electronic stethoscope was directly connected to a

portable digital recorder (Zoom H2). The accelerometer sensor was first connected to a power supply (PCB 480D06), and the accelerometer sensor and pressure sensor were connected to a pre-amplifier (Stanford Research SR560) before connecting to the recorder. Other apparatus included an adjustable stool about 18" tall and a food storage bag to protect the stethoscopes in water.

3.2.2.3 Procedure

The procedure for the second sensor comparison experiment was the same as that for the first experiment, as described in Section 3.1.1.3. The only changes were the age range of the volunteers (i.e. changed to 18-30) and the sensors being compared.

3.2.3 Data Processing

A different method of data processing was used for the second sensors experiment and is described in the following sections. It was still important to develop a method that could process all of the collected data and could quantify the heart rate and SNR.

3.2.3.1 Improve SNR

The first step in improving the SNR of the raw recording was to remove a 60-Hz component from the signal. The MATLAB iirnotch function (i.e. a second order IIR digital notch filter) with a Q factor of 35 was used; a narrow stopband was required because heart sounds would be in the same frequency range. The second step was to apply a band-pass filter in the low frequency range. A fourth order Type I Chebyshev filter with 0.05 dB of peak-to-peak ripple in the passband was used. This was to achieve a steeper roll-off, because the passbands of interest were narrow (widths around 20 Hz).

The optimal band-pass range (i.e. to improve the SNR the most) varied from recording to recording. Thus, to determine the optimal band-pass range for each recording, the spectra of the heart beat signals within a given recording was analyzed, and the filter range with a matching frequency response was found. In the last step, a Wiener filter (Zavarehei 2005) was applied to reduce the amount of noise.

3.2.3.2 Determine Heart Rate

The first step to calculate the heart rate of a given recording was to identify the individual heart beat pulses. The overall RMS voltage of the recording and the local RMS voltage for 0.034-s increments (1500 samples) were calculated. Segments where the local RMS was greater than the overall RMS were identified, and the maxima of those segments were designated as pulses.

The second step was to check for extra or missing pulses and make manual adjustments accordingly. Instantaneous heart rates were calculated using every two pulses (i.e. “lub” to “lub” and “dub” to “dub”) and were checked against the expected heart rate range. Extra pulses were removed, and missing pulses were found by identifying the maximum peak in an expected range.

3.2.3.3 Determine SNR

To calculate the SNR of a recording, the signal windows had to be distinguished from the noise. The pulses determined in the previous section were used with a spectrogram analysis to identify individual signal windows surrounding each pulse. Valid time segments were identified by overlaps in high spectrogram amplitudes in the low frequency range (0-100 Hz) and expected pulse segments determined by local RMS values. SNR was calculated as before, using Eq. (3.1). The RMS signal level was

calculated from concatenating all of the signal windows; the RMS noise level was calculated similarly, using all windows outside of the signal windows.

CHAPTER 4

RESULTS AND DISCUSSION

4.1 Sensor Comparison Experiment, v.1

The results from the first sensor comparison showed that the electronic stethoscope performed significantly better than the other sensors. The background noise was characterized and found to be comparable with typical ocean background noise. It was difficult to obtain precise measurements for the flow rate in the Lazy River, but it was estimated that the flow rate was in the general range of 10 to 35 cm/s.

4.1.1 Sensor Comparison

To compare the various sensors tested in this experiment, SNR values were calculated, and averages were analyzed in terms of sensor type, recording medium, and breathing pattern. The heart rate and SNR values for all trials are listed in Appendix A.

4.1.1.1 Acoustic Stethoscope

The acoustic stethoscope was used during three out of the nine experiments to make qualitative observations. Not surprisingly, it was easy to hear the heartbeats in air from the marked location on the ventral side for all three volunteers. From the dorsal side, no heartbeats were heard; this was expected, since suggested auscultation areas for the heart are located on the chest (Lippincott 2009). For the first experiment, all observations in the water were invalid due to water infiltration. Observations from the other two experiments showed that heartbeats were still audible in still water from the ventral side. It was possible to hear heartbeats from the ventral side in flowing water for

one of the volunteers but not the other. For all volunteers, no heart sounds were heard from the dorsal side in water.

It seems that there were no significant differences between using the stethoscope in water and using it in air when listening to the heartbeats from the ventral side. Because the observations were qualitative, it is difficult to say whether the change in medium increased or decreased the SNR.

4.1.1.2 Electronic Stethoscope

The electronic stethoscope was used in four experiments, for a total of 192 recordings. The first experiment was incomplete, because the instrument became water logged part way through testing in water. Table 4.1 shows the summary of average SNR values calculated from the autocorrelation method for the electronic stethoscope. Only two breathing patterns are shown to represent the best case (minimal lung volume for exhale-hold) and the worst case (maximum lung volume for inhale-hold).

From the ventral side, the exhale-hold recordings were comparable across environments, with average SNR values around 11 dB. On the other hand, the data for inhale-hold suggested an improved SNR in still water and flowing water. However, the standard deviation values showed that the recordings lacked consistency across experiments and trials, and it was difficult to make conclusions about the performance of the electronic stethoscope for those circumstances. From the dorsal side, there was a significant decrease in SNR compared to data from the ventral side. Among environments and breathing patterns, SNR values were low with high standard deviations, again suggesting that the data was not sufficiently repeatable.

Table 4.1: Average SNR (dB) for the electronic stethoscope.

ELECTRONIC STETHOSCOPE	Exhale-hold			Inhale-hold		
	air	water	flow	air	water	flow
Ventral	11.1	10.7	10.9	5.4	8.7	9.4
	7.0	7.3	3.7	2.7	4.7	6.3
Dorsal	2.1	2.4	1.5	1.6	1.9	3.4
	1.5	1.5	1.0	1.4	1.1	3.2

avg SNR
stdev

The recordings from the ventral side showed very clear heartbeat signals in all environments across all breathing patterns. One example recorded in air from the ventral side is shown below in Figure 4.1, showing clear lub-dub waveforms; a close-up is shown in Figure 4.2. The frequency spectra of the recording shown in Figure 4.3 shows higher levels in the range of frequencies less than 100 Hz, as expected for heartbeat sounds (Yoganathan, Gupta et al. 1976; Yoganathan, Gupta et al. 1976).

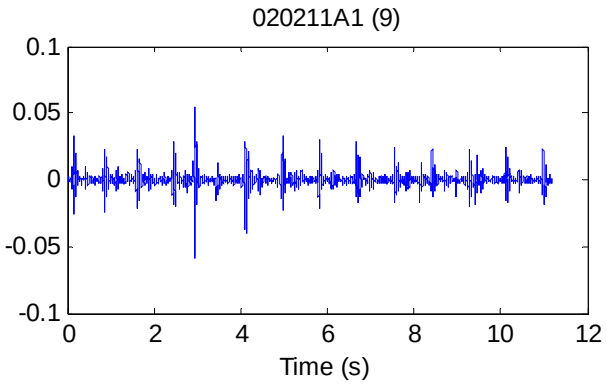

Figure 4.1: [ES] Clear heartbeat signals.

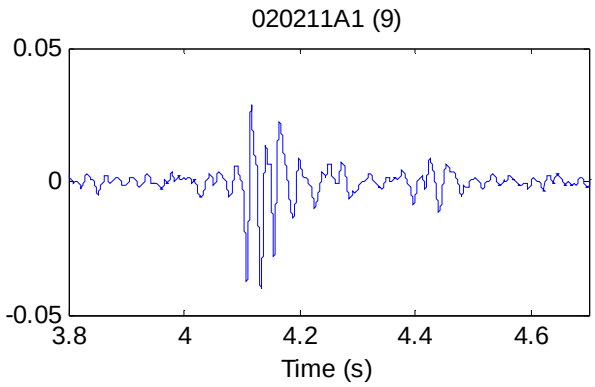

Figure 4.2: [ES] Close-up of a “lub-dub”.

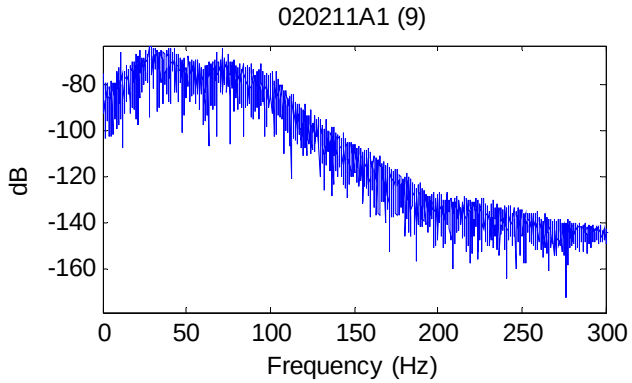

Figure 4.3: [ES] Frequency spectra.

Generally, signals were clearest for exhale-hold recordings, with decreasing clarity for normal breathing and inhale-hold. This was visible in all environments in most recordings, such as the ones shown below in Figure 4.4, recorded from the ventral side in still water. However, some experiments showed a comparable SNR across breathing patterns even in still water and flowing water, as Figure 4.5 shows examples recorded from the ventral side in flowing water.

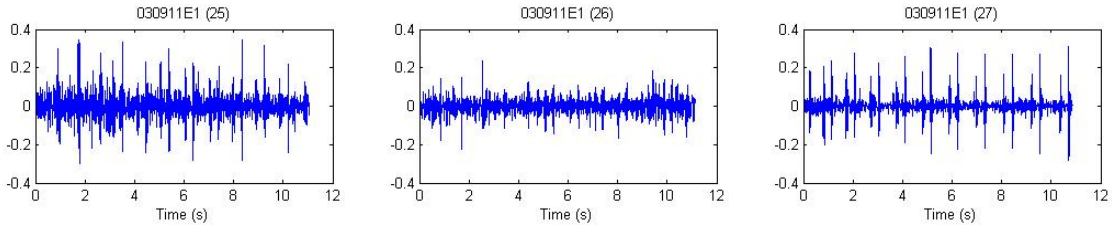

Figure 4.4: [ES, time series] Visible differences in SNR across breathing patterns. E1(25): breathing normally; E1(26): inhale-hold; E1(27): exhale-hold.

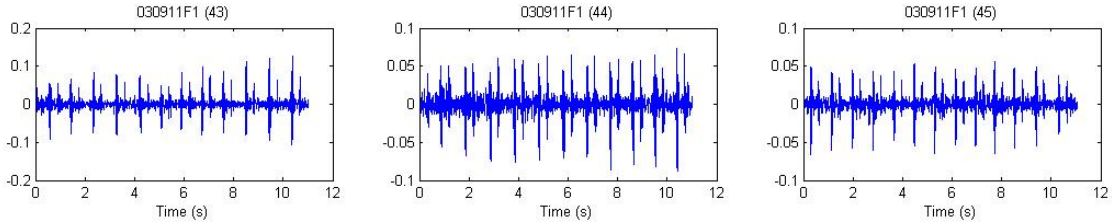

Figure 4.5: [ES, time series] Comparable SNR across breathing patterns. F1(43): breathing normally; F1(44): inhale-hold; F1(45): exhale-hold.

The recordings from the dorsal side were significantly noisier compared to those from the ventral side. Though there were peaks in the recordings, it was difficult to distinguish between heartbeats and extraneous noise, even for exhale-hold measurements. Figure 4.6 shows examples of exhale-hold recordings lacking clear heartbeat signals across all environments when recorded from the dorsal side.

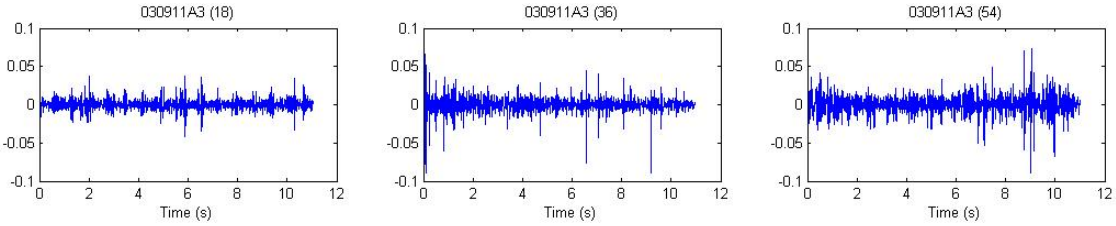

Figure 4.6: [ES, time series] Recordings from the dorsal side. A3(18): in air; A3(36): in still water; A3(54): in flowing water.

4.1.1.3 Accelerometer

The accelerometer was used in six experiments, for a total of 324 recordings. Table 4.2 below shows the summary of average SNR values calculated from the autocorrelation method for the accelerometer.

The best recordings were exhale-hold measurements taken from the ventral side in air, with an average SNR value of 5.606. The same recordings taken in water were generally also clear, but were still highly inconsistent. Other measurements – in flow, for inhale-holds, and recordings from the dorsal side – were both noisy and inconsistent.

Table 4.2: Average SNR (dB) for the accelerometer.

ACCELEROMETER	Exhale-hold			Inhale-hold		
	air	water	flow	air	water	flow
Ventral	5.6	2.9	1.8	1.9	1.2	1.4
	3.1	2.1	1.0	1.4	1.0	0.8
Dorsal	1.8	1.5	1.7	1.8	2.0	1.4
	0.8	1.5	1.3	1.1	1.4	0.8

avg SNR
stdev

Unlike the electronic stethoscope, the recordings with the accelerometer from the ventral side in air showed a large variation among experiments. Some experiments showed a noticeable difference among breathing patterns, as shown in Figure 4.7. For others, heartbeat signals could be very clear for all breathing patterns, as shown in Figure 4.8, or very noisy, as shown in Figure 4.9.

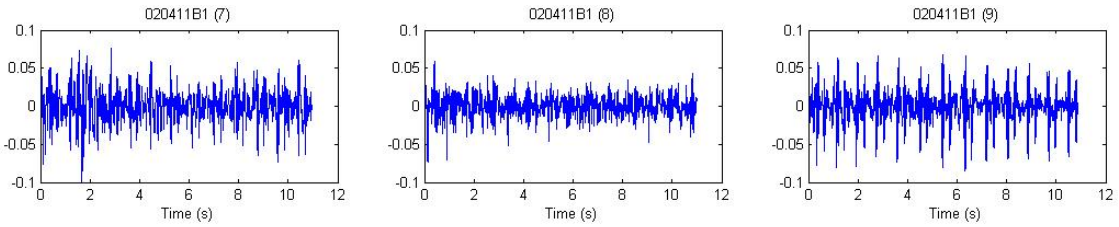

Figure 4.7: [Accel., time series] Noticeable difference among breathing patterns. B1(7): breathing normally; B1(8): inhale-hold; B1(9): exhale-hold.

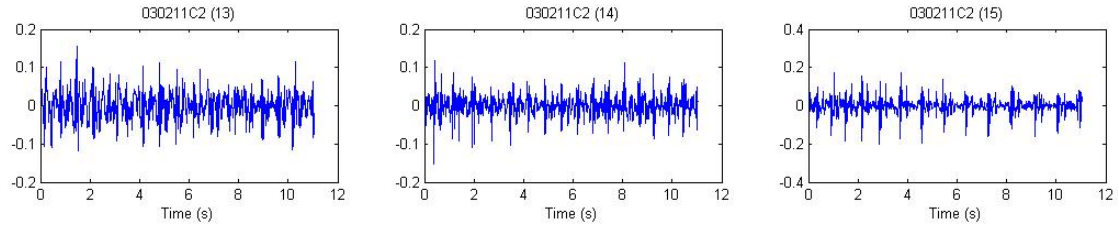

Figure 4.8: [Accel., time series] Clear heartbeats for all breathing patterns. C2(13): breathing normally; C2(14): inhale-hold; C2(15): exhale-hold.

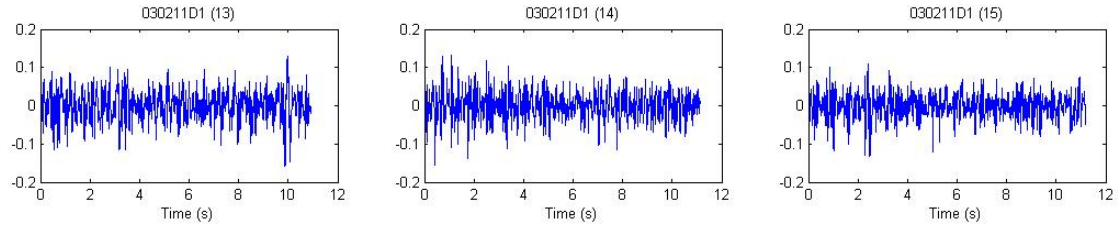

Figure 4.9: [Accel., time series] Noisy recordings for all breathing patterns. D1(13): breathing normally; D1(14): inhale-hold; D1(15): exhale-hold.

Recordings from the ventral side in still water and flowing water were similar to those taken in air but with a clear decrease in SNR. Some signals still had clear heartbeats, while other recordings were very noisy. The change in SNR from still water to flowing water was not noticeable, and similarly, it was difficult to distinguish between heartbeats and other sources of sound.

From the dorsal side, it was difficult to interpret the recordings for all environments and breathing patterns. Though the data processing extracted heart rates,

the mean and standard deviation values for the SNR suggested that the recordings were not consistent and the calculated heart rate values may not be reliable.

4.1.1.4 Hydrophone

The hydrophone was used in three experiments, for a total of 168 recordings. It should be noted that additional background noise, i.e. periodic thuds, possibly from construction outside, was present during the recordings in still water for experiment B1. Table 4.3 below shows the summary of average SNR values calculated from the autocorrelation method for the hydrophone.

Table 4.3: Average SNR (dB) for the hydrophone.

HYDROPHONE	Exhale-hold			Inhale-hold			
	air	water	flow	air	water	Flow	
Ventral	1.4	1.3	1.8	1.6	1.7	1.8	avg SNR
	0.5	0.6	1.9	0.8	1.1	1.2	stdev
Dorsal	1.3	1.4	1.2	1.4	1.5	1.7	
	0.3	0.4	0.6	0.7	1.3	0.8	

Generally, the recordings from the hydrophone were very noisy, and it was hard to visually identify heartbeats. As the SNR values also show, there were no significant changes across environments, breathing patterns, or measurements locations. However, there was also a high level of inconsistency among trials as well as experiments. Many recordings were not included in the average SNR because the calculated heart rate was not in a reasonable range.

There were also some recordings where heartbeats were relatively clear. Recordings from experiment C1 are shown below in Figure 4.10, showing signals across environments taken from the ventral side. There was a noticeable increase in SNR from

air (SNR = 1.6075) to still water (SNR = 2.4378), which makes sense, as the hydrophone is designed to operate in water. Between still water and flowing water (SNR = 2.2851), the recordings were comparable for this experiment.

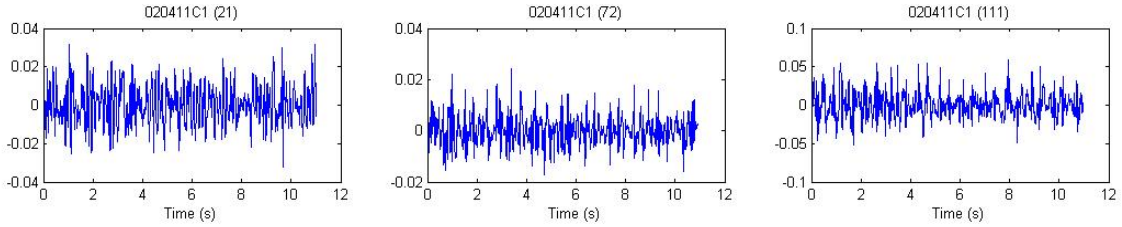

Figure 4.10: [Hydro., time series] Clear heartbeats.
C1(21): in air; C1(72): in still water; C1(111): in flowing water.

4.1.1.5 Sensor Package

The sensor package was used in five experiments, for a total of 99 recordings. The accelerometer and the hydrophone in the sensor package recorded simultaneously. Recordings were only taken from the dorsal side, because of initial plans to test the same sensor package mounted dorsally on trained dolphins. Table 4.4 below shows the summary of average SNR values calculated from the autocorrelation method for the sensor package.

Table 4.4: Average SNR (dB) for the sensor package.

Sensor Package	Exhale-hold			Inhale-hold		
	Air	water	flow	air	water	flow
PKG ACCEL	3.5	1.8	1.4	1.8	1.6	1.4
	2.1	1.4	1.0	1.7	0.9	0.5
PKG HYDRO	2.2	1.4	1.4	1.4	1.3	1.2
	1.6	0.6	0.9	0.8	0.7	0.5

avg SNR
stdev

The data was consistent with recordings taken by the sensors separately, showing that the accelerometer generally performed slightly better than the hydrophone. This was noticeable in the air for exhale-hold recordings. In other environments and for inhale-hold recordings, average SNR values were comparable. The low SNR values across all recordings were not surprising, since measurements were taken from the dorsal side.

Although both sensors were recording the same source simultaneously, many (i.e. less than half) calculated heart rates still did not match between the accelerometer and the hydrophone. Examples of matched heart rates and unmatched heart rates are shown below in Figure 4.11 and Figure 4.12 respectively. Clearly, this points to the need for improved data processing methods.

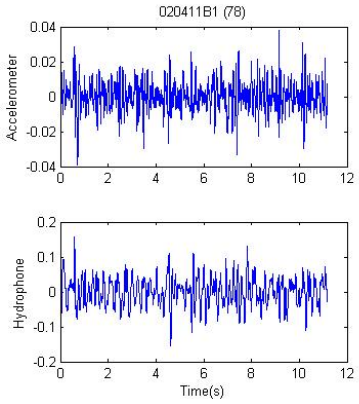

Figure 4.11: [Sensor pkg., time series] Matched heart rates.
Accelerometer: HR=65.61 bpm; Hydrophone: HR=63.19 bpm.

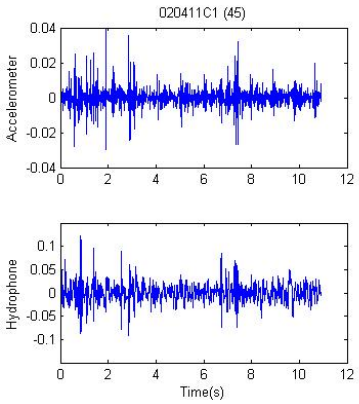

Figure 4.12: [Sensor pkg., time series] Unmatched heart rates. Accelerometer: HR=62.55 bpm; Hydrophone: HR=94.56 bpm.

4.1.1.6 Summary Comparison of Sensors

The mean SNR values averaged from the exhale-hold recordings for all experiments and trials are listed below in Table 4.5 for each sensor, recording location, and environment. Valid recordings used in the averaging were determined by a heart rate in the reasonable range (55 bpm to 100 bpm) and a positive SNR.

Table 4.5: Average SNR (dB) across experiments for exhale-hold recordings.

VENTRAL	air	water	flow
electronic stethoscope	11.1	10.7	10.9
	7.0	7.3	3.7
accelerometer	5.6	2.9	1.8
	3.1	2.1	1.0
hydrophone	1.4	1.3	1.8
	0.5	0.6	1.9

DORSAL	air	water	flow
electronic stethoscope	2.1	2.4	1.5
	1.5	1.5	1.0
accelerometer	1.8	1.5	1.7
	0.8	1.5	1.3
hydrophone	1.3	1.4	1.2
	0.3	0.4	0.6
package accelerometer	3.5	1.8	1.4
	2.1	1.4	1.0
package hydrophone	2.2	1.4	1.4
	1.6	0.6	0.9

Overall, the electronic stethoscope performed the best, across all environments and breathing patterns. From the ventral side, the electronic stethoscope was far better than the accelerometer, and the accelerometer was also noticeably better than the hydrophone. This was not surprising, since the electronic stethoscope was a product specifically designed to record clear heartbeats, with built-in signal processing, whereas the other sensors were not tailored for this application. Additionally, the rigid housing on the electronic stethoscope most likely prevented some of the transmission of background noise to the sensor. The accelerometer and the hydrophone, on the other hand, had no external housing. Looking at the nature of the single-axis accelerometer, it would have rejected noise from some directions; this may have been one of the reasons why the accelerometer performed better than the hydrophone did.

From the dorsal side, all of the sensors were comparable, with fairly low SNR. This also was not surprising; heartbeats are not usually measured from the dorsal side, because the lung creates an additional barrier between the sensor and the heart. However, there were some individual recordings that had what seemed to be exceptionally clear heartbeat signals from the dorsal side. This could be a reflection of high positional sensitivity, and it is possible that other dorsal locations would provide clearer signals. A few recordings with clear heartbeat signals are shown below in Figure 4.13, showing the electronic stethoscope and accelerometer in air and water. The sounds had a different quality from the recordings from the ventral side, which was expected, given the location of the lungs and the difference in propagation paths. It was difficult to determine if the peaks in dorsal recordings were noise or if they were actual heartbeats. There were also many recordings with high calculated SNR, but the heartbeats were still hard to identify visually. These results were promising for future work to detect heartbeat sounds from the dorsal side. Future testing and analysis may benefit from simultaneous recording from the ventral and dorsal sides to identify heartbeat sounds recorded from the dorsal side.

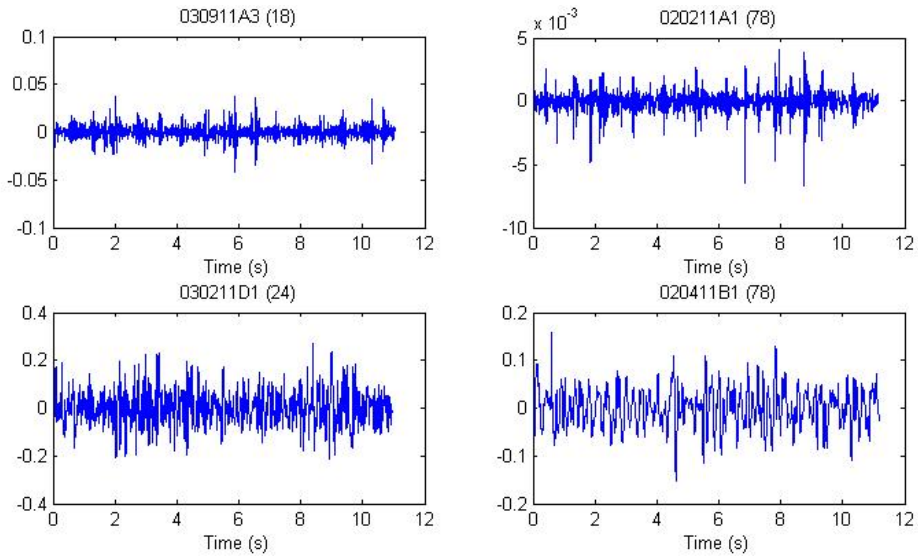

Figure 4.13: [Various, time series] Clear heartbeat signals recorded from the dorsal side. A3(18): electronic stethoscope in air; A1(78): accelerometer in still water; D1(24): sensor package accelerometer in air; B1(78): sensor package accelerometer in still water.

4.1.1.7 Problems and Sources of Error

There were some unexpected challenges during the experiment, as described below. The first attempts using the acoustic stethoscope and the electronic stethoscope revealed that the wrapped instruments were not waterproof. Corrections were made for the subsequent experimental days to better secure the instruments. An additional challenge was keeping the electronic stethoscope on to record data continuously. The device was designed to turn off after three minutes, so it became necessary to turn off and turn on the stethoscope between each trial to prevent an automatic shut-off in the middle of a recording.

Other factors may have affected the quality and reliability of the recordings. As mentioned previously, some measurements were taken with background noise present. Additionally, movement from either the volunteer or the researcher holding the sensor may also have been recorded. It was also noted that some volunteers' backs were not flat

at the marked location on the dorsal side; this meant that larger sensors such as the sensor package was not flush against the skin at all sensor locations. Lastly, for measurements in flowing water, the presence of the researcher in the water most likely affected the flow in the channel. Although the researcher stood downstream of the flow, additional flow noise may have been generated.

The greatest source of error in analyzing the results of the experiment was in the data processing. Details of the data processing methods will be presented in a later section, but the inconsistencies in the results suggest that the calculated values may not have been reliable. As shown by data presented in Appendix A, there were many instances where the heart rate values were inconsistent from trial to trial for the same volunteer in a given setup. Additionally, some of the SNR values were inconsistent with visual estimates. For some recordings, there was a high SNR calculated from the data processing, but heartbeats were not visible. On the other hand, there were also recordings with low SNR values that had visually clear heartbeats. Two examples are shown below in Figure 4.14. It is possible that the effects of bradycardia and tachycardia resulted in less accurate values calculated for the heart rate and SNR, but the inconsistencies were most likely caused by shortcomings in the data processing method used.

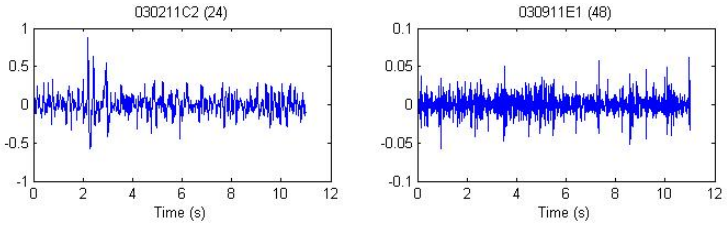

Figure 4.14: [Various, time series] Unreliable SNR values. C2(24): SNR = 6.2627, but heartbeats are not clearly visible; E1(48): SNR = -0.3413, but heartbeats are clearly present.

4.1.2 Background Noise

The background noise recordings taken by the accelerometer captured the frequency characteristics of the noise in air, still water, and flowing water. A low-pass filter was applied using the pre-amplifier (the frequency was not recorded). Figure 4.15 below shows that there were slight frequency differences among the various environments. In air, there was more noise in the higher frequencies, but in all environments, the background noise was highest in the 0-20 Hz range. That range overlaps with the frequency range of human heart beat sounds, around 10-80 Hz (Yoganathan, Gupta et al. 1976; Yoganathan, Gupta et al. 1976).

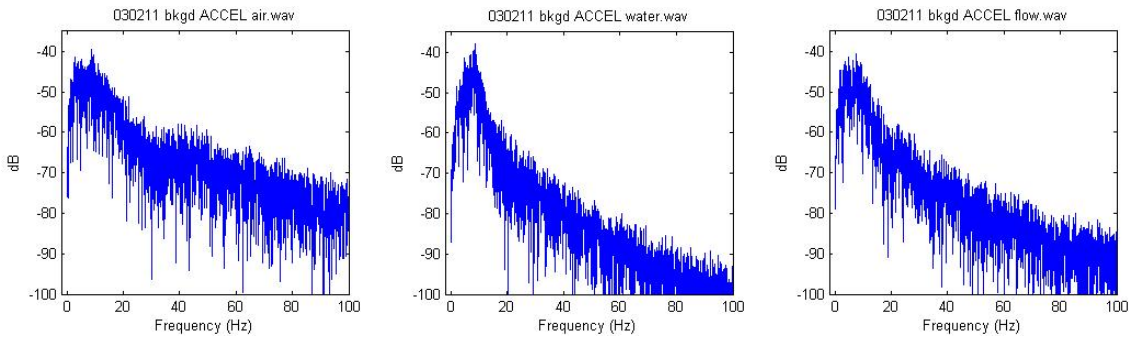

Figure 4.15: Frequency spectra of background noise.

The spectral densities of the background noise taken by the hydrophone in the sensor package are shown in Figure 4.16. The measurements from still water and flowing water are compared to a couple examples of typical deep ocean background noise, which were estimated from the Wenz curve given by Kinsler, Frey et al. (1999). As the figure shows, the background noise present in water in the first part of the experiment was either comparable or at a higher level than typical high levels of ocean noise. The frequencies of interest would be either the range of 10-80 Hz for human heart sounds (Yoganathan, Gupta et al. 1976; Yoganathan, Gupta et al. 1976) or around 10-200 Hz for cetaceans,

based on observations of trained dolphins by Miksis, Grund et al. (2001). Thus, it seems promising that if heartbeat measurements were identifiable under experimental conditions, levels of ocean background noise would not be a concern.

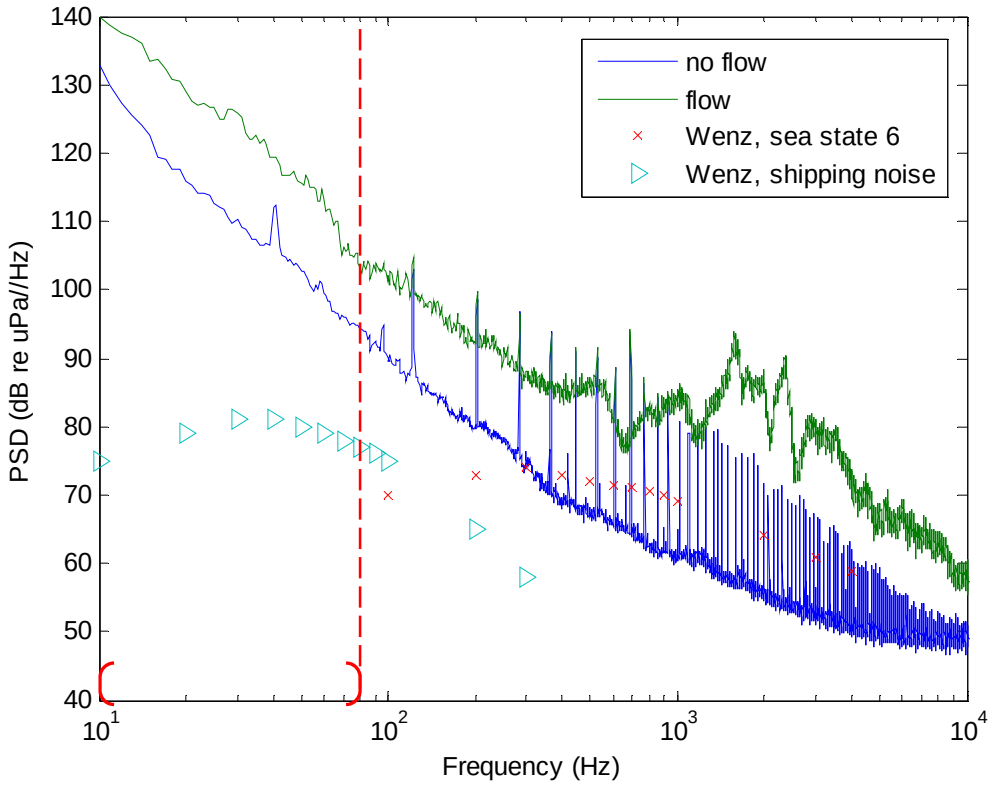

Figure 4.16: Comparison of hydrophone background noise to typical ocean noise. The red brackets and dotted red line indicate the frequency range of expected human heart sounds of 10-80 Hz.

4.1.3 Flow Rate

4.1.3.1 Aquadopp

A summary of the data taken from the Aquadopp is presented below in Table 4.6, showing the flow rate estimated to be around 9 cm/s. Because the objective was just to approximate the flow rate, the variability of average speeds among the trials was

acceptable. However, it was noted in all of the measurements that the measured speeds in the vertical direction were on the same order as the speeds in the horizontal direction. This did not match the assumption that the flow was mostly horizontal in the channel, so the second experiment to estimate the flow rate was conducted as a comparison.

Table 4.6: Summary of flow rate data from the Aquadopp.

Trial	Meas. Int. (s)	Avg. Int. (s)	Rec. time (h:mm:ss)	Avg. speed (m/s)	Std. dev. speed (m/s)
aquadropp1	2	1	0:01:46	0.10	0.037
aquadropp2	5	2	0:00:55	0.11	0.024
aquadropp3	2	1	0:00:34	0.06	0.031
aquadropp4	5	2	0:00:45	0.09	0.030
average	/	/	/	**0.09**	0.031

4.1.3.2 Floating object

The results from this part of the experiment are shown below in Table 4.7 . The speed was calculated from the time the object spent in the 6-ft section of the channel. Some measurements reflected very inaccurate flow speeds, because the object usually did not travel in a straight path; in most trials, the path curved across the channel or made loops due to flow vortices. Trial 9 was one extreme example where the object became stuck at the edge of the wall for a period of time. Using the speeds from only the straight paths (six trials out of fifteen), an average speed of 35 cm/s was found.

Table 4.7: Flow rate data from measuring floating objects.

Trial #	Object	Time (s)	Speed (m/s)
1	fishing float	7.40	0.25
2	fishing float	7.08	0.26
3	fishing float	6.90	0.27
4	fishing float	4.93	0.37
5	fishing float	7.50	0.24
6	fishing float	9.00	0.20
7	fishing float	7.98	0.23
8	orange peel	4.98	0.37
9	fishing float	17.23	0.11
10	fishing float	5.49	0.33
11	fishing float	4.56	0.40
12	fishing float	9.56	0.19
13	fishing float	9.88	0.19
14	fishing float	5.38	0.34
15	fishing float	6.39	0.29
average - "straight" paths			**0.35**
average - all paths			0.27

4.1.3.3 Possible Sources of Error

The calculated flow rates from the two different methods did not agree, most likely due to the characteristics of the flow. The experiments suggested the presence of vortices not only in the horizontal plane but also vertically. Considering the source of the flow (two vertically stacked vents located upstream, one set on both walls of the channel), the observed flow characteristics make sense. Additionally, the Aquadopp may have taken inaccurate measurements due to the setup. The sensor location was close to the surface of the water and the water itself was fairly clear. The addition of particles in the water (e.g. chlorine particles) may have helped with obtaining more accurate measurements. Using either value from the experiments, the flow rate in the river was still slow compared to the range of interested flow rates. Tyack, Johnson et al. (2006) studied dive profiles of ten free-swimming beaked whales and observed swim speeds up to around 1.7 m/s. Given that flow noise is proportional to the fourth power of flow speed

(Ko and Schloemer 1992), it should be noted that the flow noise generated by the channel underestimated flow noise conditions for whales in the ocean.

4.1.4 Data Processing

The various data processing methods are presented below with discussions on the performance of each method. Although literature suggests that an average signal and a matched filter processing successfully aids in identifying heartbeat signals (Burgess, Tyack et al. 1998), it was not the best method in this case, and the autocorrelation method was used to analyze the data from the experiments. However, there were still many inconsistencies observed, and there was a need for improved data processing methods.

4.1.4.1 Improve SNR

Three methods were used to improve SNR, as presented earlier in Section 3.1.4.1 . The first approach was to cross correlate an average heart beat signal with a full recording. The second method, autocorrelation, was to cross-correlate each recording with itself. The third method was to use a spectrogram analysis. The results of these methods are discussed below.

4.1.4.1.1 Average Signal

To determine the average signal to use for the matched filter, various windows were compared. It was observed that average signals created from longer windows (i.e. "lub-dub + noise" versus without noise) performed best. Many of the other tested windows were unsuccessful towards improving the SNR. Although this method was expected to work well, the results were unsatisfactory; SNR was slightly improved on

signals that were already clear, but there didn't seem to be a significant improvement for noisier signals.

One possible explanation for why the average signals did not improve SNR even more could be that they were not accurate representatives of "ideal" heartbeats. Each heartbeat had a different waveform, and the time between "lub" and "dub" was not necessarily constant, even during one recording for one volunteer. Additionally, there were varying characteristics of heartbeat sounds across volunteers. These factors made it difficult to create an averaged signal that truly modeled a heartbeat.

4.1.4.1.2 Autocorrelation

The autocorrelation method produced some graphs showing clear improvements in SNR, as shown below in Figure 4.17. The benefit to using autocorrelation was that it was not necessary to determine one ideal signal to use as the standard. However, there was also the assumption that there was a constant heart rate within the recording; this method would not be able to return instantaneous heart rate values.

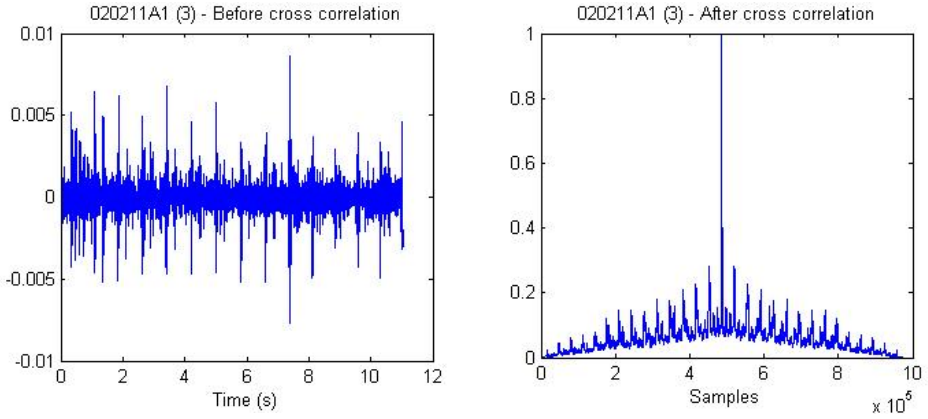

Figure 4.17: Results of the autocorrelation method.

4.1.4.1.3 Spectrogram

The spectrogram worked well for clear signals, but not any better than the original signal itself. An example of an unchanged SNR for a clear signal is shown below in Figure 4.18.

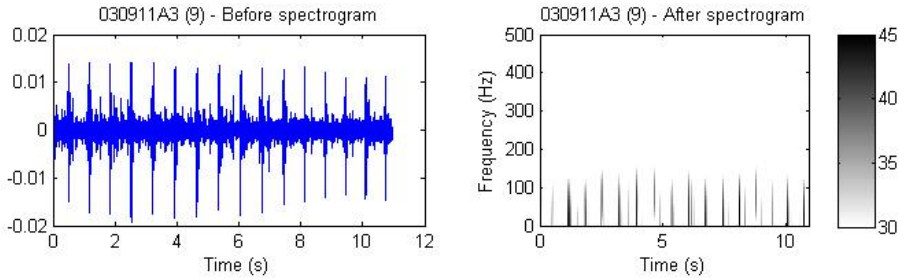

Figure 4.18: Results of the spectrogram method.

4.1.4.2 Determine Heart Rate

The heartbeats in the recordings were observed both qualitatively and quantitatively. Qualitatively, there was generally a correlation between the presence of visual and audial heartbeats, but there were some exceptions where the heartbeats were audible but not visible. Quantitative values for the heart rates were calculated from the autocorrelation method, as described previously in Section 3.1.4.2. As discussed in Section 4.1.1.7, these values often revealed inconsistencies with visual and audial estimates. Although a value for heart rate was calculated for every recording, it was not necessarily an accurate heart rate, especially if a signal had a low SNR or varying heart rates throughout one recording.

4.2 Sensor Comparison Experiment, v.2

In the second sensor comparison experiment, new sensors were designed and compared with previously existing sensors. The first section below describes the results

of sensor design testing, the second section presents the sensor comparison, and the third section discusses the data processing method used in the second sensor comparison experiment.

4.2.1 Sensor Design

4.2.1.1 Accelerometer Sensor Design

The Young's moduli of two closed cell foams were determined through experimental methods presented in Section 3.2.1. The Young's modulus for the Rubatex® 451N sample ($\rho \approx 650$ kg/m^3) was found to be 1.12×10^7 Pa, which was comparable to (i.e. on the same order of) experimental results by Guillot and Trivett (2003), where the dynamic Young's modulus approaches 3.3×10^7 Pa at low frequencies at 20°C, as shown in Figure 4.19. The Young's modulus for the Durafoam^{TM} DK1111 ($\rho \approx 73$ kg/m^3) was found to be 5.59×10^5 Pa.

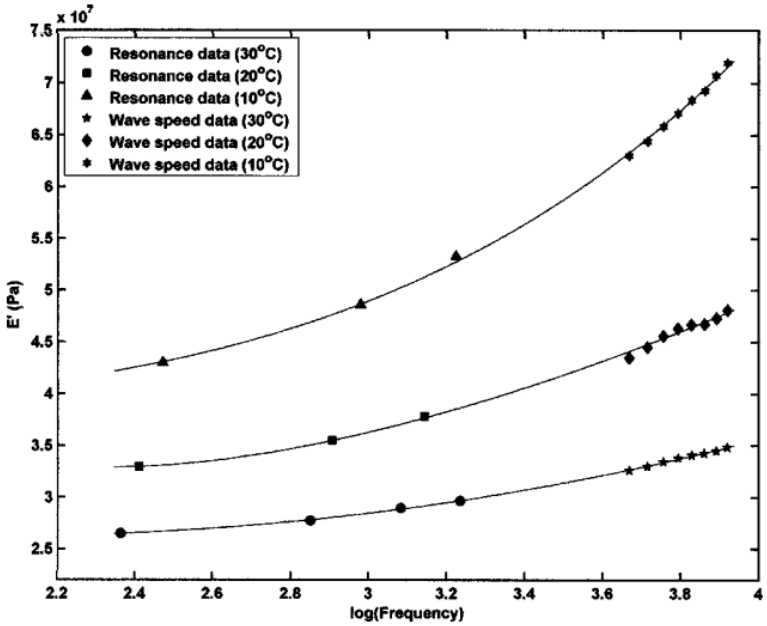

Figure 4.19: Elastic Young's Modulus of Rubatex® R451N measured at ambient pressure, as a function of temperature.
The solid lines are curve fits (Guillot and Trivett 2003).

A third material, Durafoam^{TM} DK3131 ($\rho \approx 140$ kg/m^3) was chosen as the backing material, with an estimated Young's modulus of 5×10^6 Pa, to allow for a flat low frequency response of the system. DK1111 was chosen as the surrounding material, using a more compliant material to reduce additional resistance to the motion of the accelerometer. Using a diameter of 0.020 m (0.785 in) and a height of 0.019 m (0.75 in), the spring constant was calculated to be 8.20×10^4 N/m. The total mass was determined to be 0.0042 kg. The resonance frequency of the system was at 703 Hz with a flat response in the low frequency range of 10 Hz to 100 Hz (0.176 dB difference in displacement).

To predict the standing wave resonance using Eq. (3.13), the Poisson's ratio of the Durafoam^{TM} DK3131 was needed. However, because it was difficult to determine accurately, a "worst case" resonance was calculated using v=0. Using f=100 Hz for Durafoam^{TM} DK3131, H_{res} was found to be 0.546 m, which was far greater than the

designed height. Therefore, standing wave resonance in the backing material was not a concern.

Shaker test results of the accelerometer sensor were compared to a modeled response, shown in Eq. (3.4). Figure 4.20 below shows that the experimental response deviated significantly from the model. However, it was concluded that there was a low frequency resonance component of the shaker around 40 Hz, which most likely produced the unexpected response. The shaker test appeared to reflect the shaker response rather than the frequency response of the accelerometer sensor.

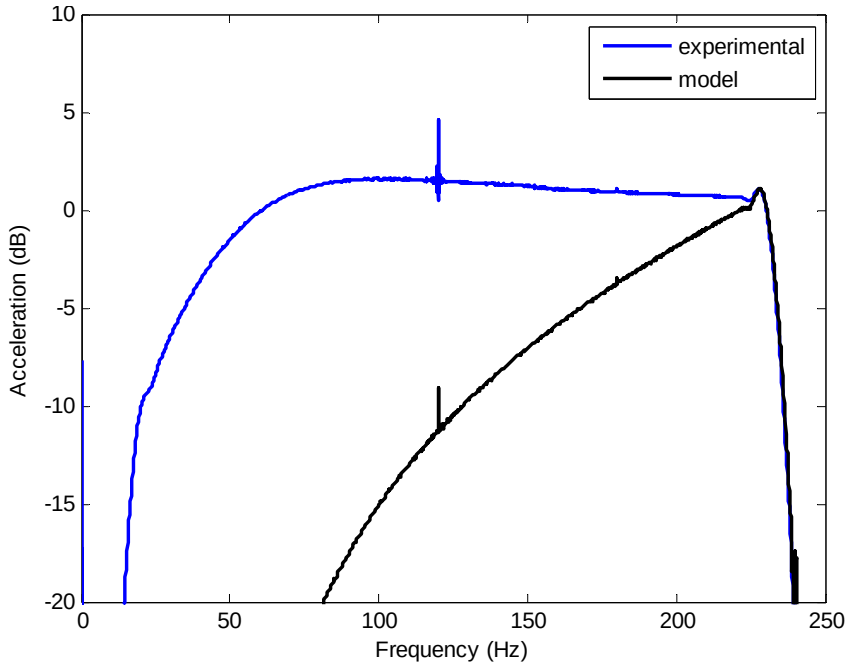

Figure 4.20: [Accel. sensor] Comparison of experimental and model shaker test results.

The accelerometer sensor was also compared to an accelerometer without housing. The shaker test results showed that the backing material did not significantly affect the performance of the accelerometer. As shown in Figure 4.21 below, there was a maximum difference of only 0.63 dB around 118 Hz (disregarding differences at 60, 120,

and 180 Hz). This also supported the conclusion that the discrepancy between the experimental and model results was due to the shaker and not the design of the accelerometer sensor itself.

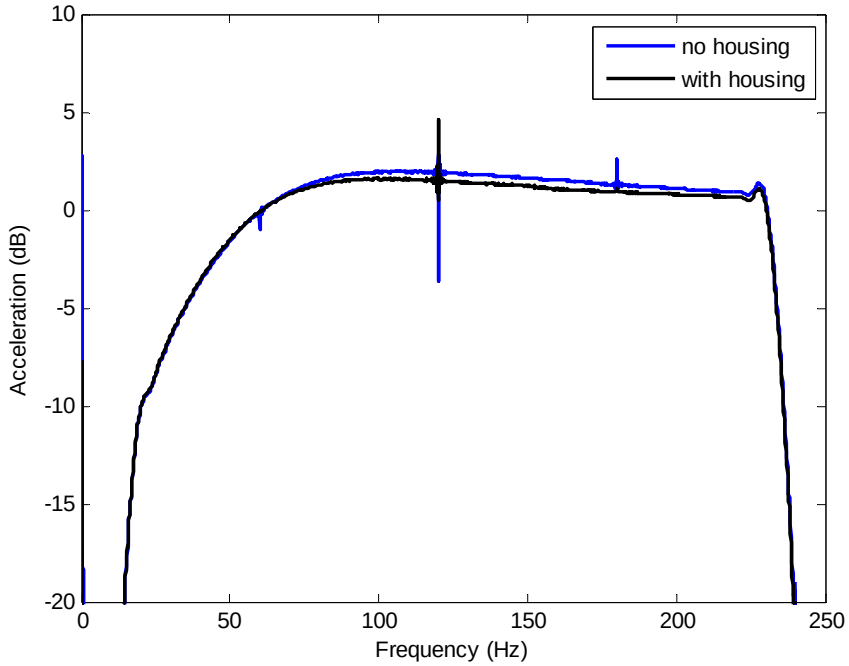

Figure 4.21: [Accel. sensor] Effect of housing on shaker test results.

4.2.1.1 Pressure Sensor Design

The spring constants of the two rubber materials were determined through an Instron machine, as described in Section 3.2.1.2. The spring constants of the silicone rubber and the Elastack were found to be 35859 N/m and 1365 N/m, respectively.

Multiple pressure sensors were tested on a shaker against a rigid surface to create a compression input. The first pressure sensor tested on the shaker was a silicone rubber core with PVDF attached with just tape. The results of one trial are shown below in Figure 4.22, showing the LDV signal from the shaker platform, the calculated displacement of the platform from the LDV signal, and the recorded output from the

PVDF. The predicted PVDF output from Eq. (3.14) was directly proportional to the input displacement, but the experimental PVDF output, as shown in the figure, did not reflect the predicted response. Instead, this showed poor coupling between the PVDF and the rubber; one side of the PVDF response matched the displacement while the other side had nearly negligible output. The promising part of the PVDF output was a high SNR value.

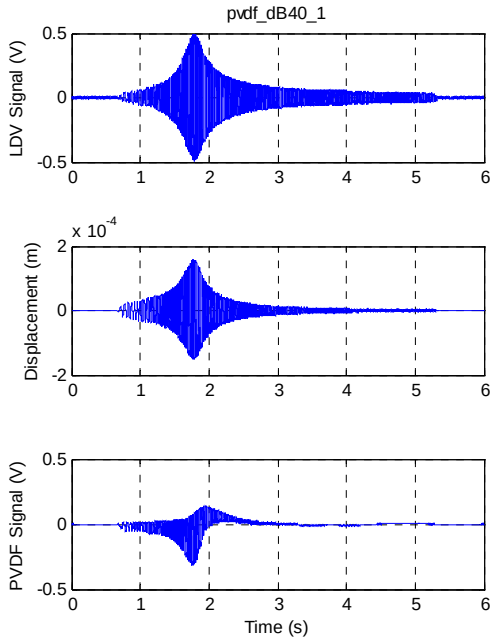

Figure 4.22: [Press. sensor] Shaker test results with poor coupling.

In the second test, the PVDF was attached to the silicone rubber core using Loctite Black Max 380. Non-linearities were observed over the range of different shaker gain settings and all of the recordings had “one-sided” responses. These were a few signs that the silicone rubber was not a good choice for the core material.

In the third test, the PVDF was attached to the Elastack rubber core using Loctite Black Max 380. The Elastack performed better than the silicone rubber over different gain settings, in that the recordings showed linear gains. Additionally, there were

symmetric responses across all gain settings, showing better coupling between the rubber and the PVDF.

The resonance frequency analysis of the shaker tests also showed that the Elastack was a better choice than the silicone rubber. The silicone rubber did not have a consistent resonance frequency over the various shaker gain settings (ranged from 60 to 73 Hz) while the Elastack had a consistent resonance frequency, which was around 32 Hz. Additionally, the experimental resonance frequency using the Elastack was a better match to the predicted resonance given in Eq. (3.16) than the resonance from the silicone rubber. Using a mass of 0.454 kg, a spring constant of 35859 N/m for the silicone rubber, 1365 N/m for the Elastack, and 15767 N/m (90 lb/in) as the shaker spring constant as listed in the manual, the resonance frequencies were calculated to be 54 Hz for the silicone rubber and 31 Hz for the Elastack.

The pressure sensors were also tested with heartbeat signals in preliminary tests on the researcher in air. After various attempts, it was found that heartbeats were both audible and visible in the recordings when the PVDF covered the entire height of the rubber core, for both the silicone rubber (with Loctite Black Max 380) and the Elastack (just tape along the vertical seam). The sensor with Elastack seemed to have a higher SNR, which could have been the result of a higher compliance, as predicted, as well as a better coupling between the PVDF and the rubber.

The final pressure sensor was constructed with the Elastack rubber covered by the PVDF, attached with tape along the vertical seam. To reduce noise at 60 Hz harmonics, shielding was added by lining the inner wall of the housing and covering the top with

copper foil. The use of battery power also significantly decreased the noise level in the sensor.

4.2.2 Sensor Comparison

To compare the various sensors tested in this experiment, SNR values were calculated using the methods described in Section 3.2.3, and averages were analyzed in terms of sensor type, recording medium, and breathing pattern. A SNR value was calculated for all 150 recordings taken from the ventral side. The same processing used on the ventral recordings was applied to dorsal recordings, but most did not have audible or visual heartbeats after processing; therefore SNR values were calculated for only a handful of dorsal recordings (i.e. 16 total). Separate results for ventral and dorsal recordings are given below, and detailed results are listed in Appendix B.

4.2.2.1 Ventral Recordings

4.2.2.1.1 Electronic Stethoscope

The electronic stethoscope was used in three experiments, for a total of 42 recordings. The second experiment was incomplete, because the instrument had a temporary malfunction at the time of testing. Table 4.8 below shows the summary of SNR values calculated for the electronic stethoscope.

Table 4.8: Average SNR (dB) for the electronic stethoscope.

E. STETH	Breathing			Inhale-hold			Exhale-hold		
	air	water	flow	air	water	flow	air	water	flow
Ventral	22.5	20.6	22.1	22.8	17.2	13.7	21.9	22.0	26.9
	4.7	6.8	10.6	6.3	4.5	7.4	3.4	2.4	5.5

avg
stdev

In air, the electronic stethoscope had comparable SNR values across the breathing patterns, which was not surprising, as the electronic stethoscope is designed to hear heartbeats in air regardless of respiratory sounds. The most consistent data was with exhale-hold, keeping with expected performance. In still water, there was some variation in the average SNR values across breathing patterns, where the exhale-hold had both the highest average and the smallest standard deviation, again in keeping with expectations. In flowing water, there was a significant difference across breathing patterns. Again, the recordings for exhale-hold were the best.

Overall, many of the electronic stethoscope recordings did not need any manual adjustments. For those that did need adjustments, most needed few corrections; adjustments were needed the most for inhale-hold recordings in flowing water. These results supported the SNR data and matched expectations. One unexpected result was a high average SNR value for recordings taken in flowing water. However, those recordings also came with greater inconsistencies, so perhaps the SNR values for flow were not as reliable.

4.2.2.1.2 Accelerometer Sensor

The accelerometer sensor was used in three experiments, for a total of 54 recordings. Table 4.9 below shows the summary of SNR values calculated for the accelerometer sensor.

Table 4.9: Average SNR (dB) for the accelerometer sensor.

ACCEL. SENSOR	Breathing			Inhale-hold			Exhale-hold		
	air	water	flow	air	water	flow	air	water	flow
Ventral	20.2	21.7	10.7	21.5	17.2	20.4	23.7	20.5	13.8
	4.8	10.8	6.4	4.6	4.4	10.0	6.7	6.2	6.5

avg
stdev

In air, the accelerometer sensor had a slighter higher SNR for exhale-hold with a slightly higher standard deviation, suggesting that it was comparable across breathing patterns. The amount of manual adjustments needed also reflected comparable performances; although inhale-hold and exhale-hold recordings had the highest SNR values, all breathing recordings did not need any manual adjustments. In still water, breathing and exhale-hold had the highest SNR, but breathing had a much higher standard deviation. One possible cause of the variation would be the inconsistent noise from respiratory sounds throughout the recordings. The accelerometer seemed to do very well with exhale-hold, as adjustments were minimal compared to other breathing situations. In flowing water, the highest average was in inhale-hold, which was surprising. However, examining manual adjustments, corrections were needed on all of the files except for one in breathing and one in exhale-hold. Therefore, the SNR data may not have been dependable. Further discussion on the effects of the manual adjustments is presented in a later section.

Looking at the SNR values across mediums, breathing and exhale-hold showed that the accelerometer sensor performed significantly worse in flowing water, as expected, whereas inhale-hold did not follow that pattern. Taking the standard deviation into consideration, the dependability of the calculated average SNR in inhale-hold in

flowing water is questionable. The exhale-hold data followed the expected pattern, with decreasing SNR from air to still water to flowing water.

4.2.2.1.3 Pressure Sensor

The pressure sensor was used in three experiments, for a total of 54 recordings. Table 4.10 below shows the summary of SNR values calculated for the pressure sensor.

Table 4.10: Average SNR (dB) for the pressure sensor.

PRESS. SENSOR	Breathing			Inhale-hold			Exhale-hold		
	air	water	flow	air	water	flow	air	water	flow
Ventral	18.5	19.9	16.5	27.3	15.8	16.2	20.6	19.4	22.9
	6.5	9.3	4.0	6.8	4.1	5.6	8.6	4.5	7.6

avg
stdev

In air, there was a significantly higher SNR for inhale-hold, with similar standard deviations across breathing patterns, which was an unexpected result. Looking at manual corrections, breathing and exhale-hold required the least adjustments, while inhale-hold recordings needed a significant amount of adjusting. Figure 4.23 below shows an example of a recording with a high calculated SNR but actually unclear heartbeats.

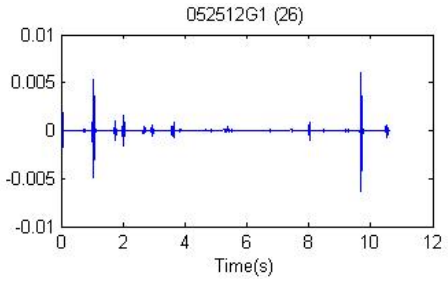

Figure 4.23: High SNR for an unclear recording.

In still water and flowing water, the results generally matched expectations, with better results in exhale-hold. As anticipated, almost all of the flow recordings required

manual adjustments. Across air, still water, and flowing water, the data did not follow the expected trend of decreasing performance; no conclusions were made for which medium allowed the highest SNR. Overall, with inconsistent SNR values and considerable adjustments, it was difficult to draw definite conclusions with the pressure sensor.

4.2.2.1.4 Summary of Ventral Recordings

The mean SNR values for all experiments and trials where recordings were taken from the ventral side are listed below in Table 4.11 for each sensor, breathing pattern, and environment.

Table 4.11: Average SNR (dB) for all ventral recordings.

Ventral	Breathing			Inhale-hold			Exhale-hold		
	air	water	flow	air	water	flow	air	water	flow
E. STETH	22.5	20.6	22.1	22.8	17.2	13.7	21.9	22.0	26.9
	4.7	6.8	10.6	6.3	4.5	7.4	3.4	2.4	5.5
ACCEL. SENSOR	20.2	21.7	10.7	21.5	17.2	20.4	23.7	20.5	13.8
	4.8	10.8	6.4	4.6	4.4	10.0	6.7	6.2	6.5
PRESS. SENSOR	18.5	19.9	16.5	27.3	15.8	16.2	20.6	19.4	22.9
	6.5	9.3	4.0	6.8	4.1	5.6	8.6	4.5	7.6

avg
stdev

All average SNR values were very high for the ventral recordings. There was a general increase in SNR from the first sensor comparison experiment as a result of data processing methods, as discussed in a later section. Comparing the SNR of the sensors to one another, the results from the accelerometer sensor generally matched those from the electronic stethoscope and were slightly better than those from the pressure sensor in air and still water. However, in flowing water, there was a significant difference in performance of the accelerometer sensor. The pressure sensor, which was modeled after the electronic stethoscope, generally performed only slightly worse than the electronic

stethoscope did. This most likely reflected the difference in refinement between the two sensors.

4.2.2.2 Dorsal Recordings

From the 150 recordings taken from the dorsal side, SNR values were calculated for only 16 files. The summary of the dorsal side recordings is shown below in Table 4.12.

Table 4.12: Average SNR (dB) for dorsal recordings.

Dorsal	Breathing			Inhale-hold			Exhale-hold		
	air	water	flow	air	water	flow	air	water	flow
E. STETH	22.5	n/a	n/a	n/a	n/a	n/a	19.1	n/a	n/a
	9.2	n/a	n/a	n/a	n/a	n/a	5.9	n/a	n/a
ACCEL. SENSOR	11.8	n/a	n/a	36.4	n/a	n/a	17.2	n/a	n/a
	n/a	n/a	n/a	n/a	n/a	n/a	8.6	n/a	n/a
PRESS. SENSOR	7.7	n/a	n/a	n/a	n/a	n/a	20.8	n/a	n/a
	0.7	n/a	n/a	n/a	n/a	n/a	7.1	n/a	n/a

avg
stdev

It was expected that some recordings would have clear heartbeats in still water, but the only recordings with clear heartbeats were in air. The results across breathing were as expected: only one recording in inhale-hold had clear heartbeats; there were five recordings with breathing and ten recordings with exhale-hold.

All recordings required manual adjustments in identifying heartbeats (either deleting extra pulses or filling in missing pulses), and almost all required a significant amount of adjustments. With breathing recordings, it seemed that there was a significant difference across sensors, where the electronic stethoscope performed the best and the pressure sensor performed the worst. However, with exhale-hold recordings, the sensors

were more evenly matched, with the pressure sensor, in fact, performing slightly better than the electronic stethoscope did.

4.2.2.3 Summary

Ultimately, for application purposes, the designed sensor needs to work in the water, with and without the presence of flow noise. From the ventral recordings, in still water, all of the sensors were comparable, and in flowing water, the accelerometer sensor seemed the worse (not taking the inhale-hold into consideration). This suggests that a transducer like the electronic stethoscope or pressure sensor would be the best choice. However, there were a few instances where there was a higher SNR in flowing water than in still water. This unexpected trend brings the validity of the data from flowing water into question.

None of the dorsal recordings in water had clear heartbeats. Therefore, based on the ventral data in water and the dorsal data in air, the recommended sensor would be an electronic stethoscope or another form of an improved pressure sensor. Even so, the results showed that an accelerometer sensor may still work well. As there are many different approaches to the design solution, it seems that all methods in this experiment have the potential to succeed.

4.2.2.4 Problems and Sources of Error

There were a few factors that may have affected the recordings. As in the first sensors experiment, some data were taken with additional background noise (i.e. people present at the pool). The presence of the researcher in the water again affected the flow in the channel for measurements taken in flowing water.

It was noted that some recordings for volunteer H1 had much lower SNR values when compared to other volunteers' SNR values under the same circumstances. One possible cause is that there was a lower heartbeat signal level due to the volunteer's anatomy, though there were no clear observable differences during the experiment. It is also possible that conditions during the experiment were different, whether it was inconsistencies with the researcher positioning the sensor or increased background noise levels.

Lastly, manual adjustments may have had an effect on SNR results. Human bias was present in identifying pulses, i.e. the natural tendency is to look for peaks. Therefore, non-heartbeats may have been chosen as heartbeats, and the resulting SNR values may have been increased.

4.2.3 Data Processing

The first step in improving the SNR of the recordings, taking out a 60-Hz component, improved some recordings more than others. The first substantial improvement came from the band-pass filter; the SNR increased significantly when the correct band-pass range was chosen. The ranges varied across all of the recordings; some were in the 30-40 Hz range, while others were around 70-80 Hz. The second significant improvement came from the Wiener filter, which worked extremely well with signals that already had clear heartbeats. The Wiener filter did not help in identifying missing heartbeats.

This data processing method was found to be better than the one used in the first sensors experiment. However, it was not as robust as it was anticipated to be, and manual checks and adjustments were still necessary in identifying heartbeats. This method also

required all heartbeats to be detectable in order to calculate a SNR value, which meant most of the dorsal recordings were unquantifiable.

The method used in this sensor experiment also improved the SNR data for the first sensor experiment. Recordings for the accelerometer and the hydrophone were cleaned up, making them more comparable to the electronic stethoscope than they were previously. This shows the importance of developing an optimized method to improve the recordings.

CHAPTER 5

CLOSING

Two experiments were conducted to compare the performance of various sensors in detecting heart rate under water. The first sensor experiment tested an electronic stethoscope, an accelerometer, and a hydrophone. The electronic stethoscope performed the best and the hydrophone performed the worst, with significant differences in the SNR values of recordings taken from the ventral side. All recordings from the dorsal side had low SNR values, and there was not a sensor that clearly performed best. The second sensor experiment tested an electronic stethoscope, a customized accelerometer sensor, and a customized pressure sensor. The electronic stethoscope still performed better than the other sensors, but it was only slightly better. All of the sensors had high SNR values in the ventral recordings; improved data processing methods contributed significantly to high SNR values. From the dorsal side, there were only a few recordings with clear heartbeats.

If the work presented in this thesis was to be repeated or studied further, there are some recommendations for the sensor comparison experiments. Because it was generally difficult to identify heartbeats for the dorsal recordings, it would be helpful to have an additional sensor recording simultaneously, e.g. recording ventral and dorsal heart sounds simultaneously or even recording EKG data and dorsal heart sounds simultaneously. Recording ambient temperatures would also be helpful to study the effect of changes in environment on heart rate. For data processing, another method to improve SNR would be to use a combination of the two versions presented; after applying the band-pass filter

and the Wiener filter, autocorrelation would be applied. Specifically for the sensor package, an additional data processing method would be correlating the recording of the accelerometer with the recording of the hydrophone. Lastly, other data processing methods could be used, such as classification algorithms available through bioacoustics analysis software (CIMRS Bioacoustics Lab 2010).

The next step towards designing a heart rate monitor is to look at additional design challenges, as they will most likely affect the performance of the sensors and create clearer differences. The results from the experiments on human subjects were only preliminary indicators. One problem with using humans as models for cetaceans comes from a difference in geometry due to anatomy; the distance between the sensor and the heart will be much greater with cetaceans. Future experiments include testing sensors in water with a whale model to examine the effects of positioning the sensor, for both still water and flow situations. Subsequent experiments would test sensors on trained animals, also for static and flow noise situations. Additionally, improvements in data processing are needed to match the needs of the final sensor design. The processing must be rigorous enough for all heart rate ranges, ideally with the capability to return instantaneous heart rates.

There are many long term challenges to consider for the device. Waterproofing was clearly an issue in the experiments conducted in shallow water and will continue to be a challenge. The device also must be able to survive great depths, and, hopefully, to function at those depths. The hydrostatic pressure may affect both the waterproofing as well as the transducer response due to the stiffening of the compliant materials. Other challenges include a method to power the device, on-board data processing as well as sufficient data storage, and designing an effective non-invasive attachment method.

Clearly, there is much work to do towards the design of a heart rate monitor for free-swimming cetaceans, but the results from these preliminary steps in this project show promising progress towards this goal.

APPENDIX A

DATA FROM SENSOR COMPARISON EXPERIMENT, V.1

Table A.1: Data for exhale-hold recordings from the ventral side.

EXHALE	Name	HR	SNR			Name	HR	SNR			Name	HR	SNR	
ES front air	'020211A1 (3)'	78.53	8.81		**ES front water**	'020211A1 (57)'	75.70	0.55		**ES front flow**	'030911E1 (39)'	63.04	5.21	
	'020211A1 (9)'	70.77	2.91			'020211A1 (63)'	83.95	0.41			'030911E1 (45)'	55.93	11.76	x
SNR mean	'020211A1 (15)'	80.05	18.18		**SNR mean**	'030911E1 (21)'	55.06	3.70		**SNR mean**	'030911E1 (51)'	59.92	12.05	
11.09	'030911E1 (3)'	80.75	3.63		10.71	'030911E1 (27)'	56.13	7.97		10.92	'030911F1 (39)'	72.42	14.82	
	'030911E1 (9)'	97.22	3.97			'030911E1 (33)'	56.10	8.03			'030911F1 (45)'	72.24	12.22	
SNR stdev	'030911E1 (15)'	86.69	4.69		**SNR stdev**	'030911F1 (21)'	69.54	19.40		**SNR stdev**	'030911F1 (51)'	72.74	15.86	
7.04	'030911F1 (3)'	75.27	4.60		7.26	'030911F1 (27)'	65.80	19.24		3.69	'030911A3 (39)'	62.69	10.61	
	'030911F1 (9)'	77.87	18.99			'030911F1 (33)'	69.92	20.09			'030911A3 (45)'	70.79	10.03	
	'030911F1 (15)'	70.04	17.29			'030911A3 (21)'	64.21	13.84			'030911A3 (51)'	77.40	6.56	
	'030911A3 (3)'	90.07	17.55			'030911A3 (27)'	66.67	11.03						
	'030911A3 (9)'	87.21	20.55			'030911A3 (33)'	67.15	13.53						
	'030911A3 (15)'	84.20	11.89											
ACCEL front air	'020211A1 (21)'	82.42	11.75		**ACCEL front water**	'020211A1 (69)'	57.99	2.09		**ACCEL front flow**	'020211A1 (105)'	55.37	2.51	
	'020211A1 (27)'	76.13	5.81			'020211A1 (75)'	56.77	1.71			'020211A1 (111)'	72.89	0.80	
SNR mean	'020211A1 (33)'	72.81	7.39		**SNR mean**	'020211A1 (81)'	88.90	1.08		**SNR mean**	'020211A1 (117)'	66.63	1.64	
5.61	'020411B1 (3)'	67.08	4.37		2.91	'030211A2 (30)'	70.03	1.35		1.84	'020411B1 (81)'	65.01	0.55	
	'020411B1 (9)'	70.88	7.95			'030211A2 (36)'	74.07	0.82			'020411B1 (87)'	66.65	4.45	
SNR stdev	'020411B1 (15)'	73.15	7.28		**SNR stdev**	'030211A2 (42)'	91.94	3.60		**SNR stdev**	'020411B1 (93)'	58.74	3.64	
3.10	'020411C1 (3)'	68.53	5.67		2.07	'020411B1 (42)'	58.04	5.13		1.05	'020411C1 (87)'	66.70	0.97	
	'020411C1 (9)'	65.03	6.31			'020411B1 (48)'	60.52	6.26			'020411C1 (93)'	65.04	1.44	
	'020411C1 (15)'	60.84	6.05			'020411B1 (54)'	56.48	7.00			'020411C1 (99)'	65.25	1.42	
	'030211D1 (3)'	88.47	3.62			'020411C1 (48)'	63.33	2.57			'030211D1 (57)'	94.13	2.25	
	'030211D1 (9)'	85.45	2.12			'020411C1 (54)'	62.47	0.73			'030211D1 (63)'	72.22	1.27	
	'030211D1 (15)'	72.12	2.32			'020411C1 (60)'	87.55	1.39			'030211D1 (69)'	61.27	1.60	
	'030211C2 (3)'	70.62	10.24			'030211C2 (30)'	Invalid(54.49)	5.72	x		'030211C2 (57)'	62.53	1.27	
	'030211C2 (9)'	69.82	8.36			'030211C2 (36)'	62.17	4.20			'030211C2 (63)'	63.02	2.94	
	'030211C2 (15)'	67.35	7.23			'030211C2 (42)'	63.32	5.91			'030211C2 (69)'	62.68	2.70	
	'030211A2 (3)'	94.17	0.25			'030211D1 (30)'	61.79	2.60			'030211A2 (57)'	59.93	1.10	
	'030211A2 (9)'	62.79	2.17			'030211D1 (36)'	70.64	0.72			'030211A2 (63)'	87.95	0.90	
	'030211A2 (15)'	67.37	2.03			'030211D1 (42)'	60.09	2.25			'030211A2 (69)'	77.12	1.69	
HYDRO front air	020211A1 (39)'	66.75	1.61		**HYDRO front water**	'020211A1 (87)'	56.60	1.48		**HYDRO front flow**	'020211A1 (123)'	78.82	0.04	
	'020211A1 (45)'	67.50	1.72			'020211A1 (93)'	78.32	1.03			'020211A1 (129)'	59.69	0.92	
SNR mean	'020211A1 (51)'	74.89	1.11		**SNR mean**	'020211A1 (99)'	88.96	1.07		**SNR mean**	'020211A1 (135)'	83.67	1.04	
1.42	'020411B1 (21)'	64.54	1.42		1.27	'020411B1 (60)'	68.87	1.37		1.75	'020411B1 (99)'	94.57	2.05	
	'020411B1 (27)'	91.98	1.53			'020411B1 (66)'	79.73	0.52			'020411B1 (105)'	57.92	6.02	
SNR stdev	'020411B1 (33)'	61.84	0.47		**SNR stdev**	'020411B1 (72)'	83.75	0.83		**SNR stdev**	'020411B1 (111)'	Invalid (105.69)	0.84	x
0.52	'020411C1 (21)'	69.89	1.61		0.57	'020411C1 (66)'	Invalid (54.28)	2.13	x	1.87	'020411C1 (105)'	59.73	0.81	
	'020411C1 (27)'	85.07	1.39			'020411C1 (72)'	64.37	2.44			'020411C1 (111)'	63.92	2.29	
	'020411C1 (33)'	58.05	2.41			'020411C1 (78)'	67.66	1.40			'020411C1 (117)'	64.60	0.87	
	'020411C1 (39)'	79.76	0.91											

Table A.2: Data for exhale-hold recordings from the dorsal side.

EXHALE	Name	HR	SNR			Name	HR	SNR			Name	HR	SNR	
ES back air	'020211A1 (6)'	56.68	-1.35	x	**ES back water**	'020211A1 (60)'	65.34	5.18		**ES back flow**	'030911E1 (42)'	68.64	0.67	
	'020211A1 (12)'	89.71	0.54			'020211A1 (66)'	84.34	3.38	x		'030911E1 (48)'	80.91	-0.34	x
SNR mean	'020211A1 (18)'	55.44	1.60		**SNR mean**	'030911E1 (24)'	67.15	0.90		**SNR mean**	'030911E1 (54)'	55.19	2.06	
2.09	'030911E1 (6)'	76.36	2.65		2.41	'030911E1 (30)'	56.33	2.15		1.46	'030911F1 (42)'	81.14	0.98	
	'030911E1 (12)'	69.46	4.11			'030911E1 (36)'	72.99	1.27			'030911F1 (48)'	75.25	0.31	
SNR stdev	'030911E1 (18)'	79.75	3.10		**SNR stdev**	'030911F1 (24)'	69.60	0.43		**SNR stdev**	'030911F1 (54)'	59.21	0.85	
1.53	'030911F1 (6)'	95.43	-0.05	x	1.52	'030911F1 (30)'	66.36	2.76		0.96	'030911A3 (42)'	73.81	1.31	
	'030911F1 (12)'	99.39	0.56			'030911F1 (36)'	59.26	-0.88	x		'030911A3 (48)'	71.90	2.53	
	'030911F1 (18)'	58.07	1.75			'030911A3 (24)'	70.72	2.67			'030911A3 (54)'	64.30	2.99	
	'030911A3 (6)'	87.40	1.39			'030911A3 (30)'	84.15	2.19						
	'030911A3 (12)'	68.39	0.41			'030911A3 (36)'	79.19	4.14						
	'030911A3 (18)'	86.65	4.79											
ACCEL back air	'020211A1 (24)'	62.51	2.29		**ACCEL back water**	'020211A1 (72)'	61.51	3.01		**ACCEL back flow**	'020211A1 (108)'	59.91	2.42	
	'020211A1 (30)'	Invalid (53.85)	3.14	x		'020211A1 (78)'	61.39	5.74			'020211A1 (114)'	73.86	4.98	
SNR mean	'020211A1 (36)'	74.63	3.49		**SNR mean**	'020211A1 (84)'	88.21	1.15		**SNR mean**	'020211A1 (120)'	91.00	1.90	
1.84	'020411B1 (6)'	59.97	1.53		1.53	'020411B1 (45)'	Invalid (103.77)	2.03	x	1.71	'020411B1 (84)'	69.11	0.73	
	'020411B1 (12)'	62.46	2.13			'020411B1 (51)'	Invalid (102.00)	1.67	x		'020411B1 (90)'	64.70	3.68	
SNR stdev	'020411B1 (18)'	62.18	0.57		**SNR stdev**	'020411B1 (57)'	68.28	0.21		**SNR stdev**	'020411B1 (96)'	90.53	1.12	
0.77	'020411C1 (6)'	77.73	0.62		1.48	'020411C1 (51)'	93.45	0.46		1.33	'020411C1 (90)'	94.41	1.77	
	'020411C1 (12)'	61.98	2.67			'020411C1 (57)'	63.24	1.01			'020411C1 (96)'	56.63	3.27	
	'020411C1 (18)'	85.37	1.64			'020411C1 (63)'	76.56	1.57			'020411C1 (102)'	Invalid (100.71)	1.07	x
	'030211D1 (6)'	62.32	-0.39	x		'030211D1 (33)'	78.74	2.91			'030211D1 (60)'	Invalid (101.28)	0.97	x
	'030211D1 (12)'	92.82	1.21			'030211D1 (39)'	72.18	1.07			'030211D1 (66)'	70.01	0.91	
	'030211D1 (18)'	72.18	1.74			'030211D1 (45)'	61.77	1.11			'030211D1 (72)'	82.34	0.13	
	'030211C2 (6)'	64.39	1.84			'030211C2 (33)'	72.01	0.37			'030211C2 (60)'	95.15	2.14	
	'030211C2 (12)'	86.73	2.32			'030211C2 (39)'	75.52	0.43			'030211C2 (66)'	90.53	1.30	
	'030211C2 (18)'	58.94	1.18			'030211C2 (45)'	Invalid (101.99)	2.95	x		'030211C2 (72)'	79.39	0.45	
	'030211A2 (6)'	68.59	2.08			'030211A2 (33)'	86.65	0.61			'030211A2 (60)'	62.65	0.40	
	'030211A2 (12)'	68.80	1.47			'030211A2 (39)'	70.78	0.76			'030211A2 (66)'	92.72	1.38	
	'030211A2 (18)'	99.67	2.61			'030211A2 (45)'	97.68	2.59			'030211A2 (72)'	87.97	0.84	
HYDRO back air	'020211A1 (42)'	80.27	1.49		**HYDRO back water**	'020211A1 (90)'	95.83	1.20		**HYDRO back flow**	'020211A1 (126)'	Invalid (101.25)	0.99	x
	'020211A1 (48)'	Invalid (54.05)	0.86	x		'020211A1 (96)'	58.82	2.36			'020211A1 (132)'	73.58	1.13	
SNR mean	'020211A1 (54)'	84.16	1.14		**SNR mean**	'020211A1 (102)'	84.16	1.56		**SNR mean**	'020211A1 (138)'	56.84	2.27	
1.30	'020411B1 (24)'	Invalid (100.98)	0.59	x	1.44	'020411B1 (63)'	96.13	1.22		1.21	'020411B1 (102)'	63.36	0.85	
	'020411B1 (30)'	68.73	1.11			'020411B1 (69)'	67.98	1.28			'020411B1 (108)'	55.55	-0.27	x
SNR stdev	'020411B1 (36)'	Invalid (100.20)	0.26	x	**SNR stdev**	'020411B1 (75)'	Invalid (53.13)	2.00	x	**SNR stdev**	'020411B1 (114)'	95.36	0.93	
0.33	'020411C1 (24)'	70.99	1.92		0.44	'020411C1 (69)'	79.52	1.06		0.57	'020411C1 (108)'	Invalid (106.90)	1.58	x
	'020411C1 (30)'	69.64	1.41			'020411C1 (75)'	Invalid (54.87)	3.60	x		'020411C1 (114)'	73.69	1.39	
	'020411C1 (36)'	95.52	1.07			'020411C1 (81)'	72.88	1.41			'020411C1 (120)'	64.48	0.71	
	'020411C1 (42)'	87.02	0.97											

Table A.3: Data for exhale-hold recordings for the sensor package.

EXHALE		HR		SNR			
	Name	accelometer	hydrophone	accelometer	hydrophone	ac	hy
HYDRO/ACCEL	'020411B1 (39)'	65.42	Invalid (106.61)	2.69	2.47		x
exhale hold	'020411C1 (45)'	62.55	94.56	3.68	2.45		
air	'030211D1 (21)'	76.39	58.87	1.92	1.67		
	'030211D1 (24)'	72.45	98.18	8.77	1.52		
	'030211D1 (27)'	66.45	65.25	3.34	1.86		
	'030211C2 (21)'	62.64	58.00	4.79	1.94		
	'030211C2 (24)'	59.79	85.56	4.21	6.26		
	'030211C2 (27)'	58.69	63.14	4.43	0.85		
	'030211A2 (21)'	55.52	58.25	2.03	2.47		
	'030211A2 (24)'	75.47	83.19	1.57	1.19		
	'030211A2 (27)'	69.33	62.79	1.45	-0.20		x
			mean	3.53	2.25		
			stdev	2.10	1.60		
HYDRO/ACCEL	'020411B1 (78)'	65.61	63.19	3.81	1.05		
exhale hold	'020411C1 (84)'	59.61	75.22	0.92	2.46		
still water	'030211D1 (48)'	65.17	60.03	0.19	1.98		
	'030211D1 (51)'	61.03	Invalid (105.98)	1.21	0.99		x
	'030211D1 (54)'	63.19	98.92	0.20	1.21		
	'030211C2 (48)'	71.64	71.45	0.23	1.68		
	'030211C2 (51)'	62.46	78.65	1.44	1.63		
	'030211C2 (54)'	78.30	69.00	3.64	0.60		
	'030211A2 (48)'	65.69	80.27	3.83	1.24		
	'030211A2 (51)'	57.88	58.22	2.35	1.39		
	'030211A2 (54)'	59.28	57.53	2.00	0.69		
			mean	1.80	1.39		
			stdev	1.44	0.57		
HYDRO/ACCEL	'020411B1 (117)'	58.88	90.28	1.77	0.70		
exhale hold	'020411C1 (123)'	55.91	58.22	0.63	-1.48		x
flowing water	'030211D1 (75)'	93.73	70.32	0.99	2.94		
	'030211D1 (78)'	93.46	68.40	1.97	2.59	x	x
	'030211D1 (81)'	Invalid (101.13)	98.88	2.60	1.31	x	x
	'030211C2 (75)'	94.39	88.69	2.28	0.97		
	'030211C2 (78)'	85.32	55.73	0.84	0.59		
	'030211C2 (81)'	93.79	90.21	0.71	1.02		
	'030211A2 (75)'	73.98	88.82	0.81	2.50		
	'030211A2 (78)'	58.91	97.20	0.90	1.74		
	'030211A2 (81)'	87.58	94.01	3.58	0.84		
			mean	1.39	1.41		
			stdev	0.99	0.88		

Table A.4: Data for inhale-hold recordings from the ventral side.

INHALE	Name	HR	SNR			Name	HR	SNR			Name	HR	SNR	
ES front air	'020211A1 (2)'	68.06	2.56		**ES front water**	'020211A1 (56)'	61.04	5.55		**ES front flow**	'030911E1 (38)'	61.96	2.03	
	'020211A1 (8)'	73.38	4.48			'020211A1 (62)'	Invalid (100.58)'	42.79	x		'030911E1 (44)'	61.03	1.25	
SNR mean	'020211A1 (14)'	57.25	3.22		**SNR mean**	'030911E1 (20)'	Invalid (100.51)'	0.93	x	**SNR mean**	'030911E1 (50)'	74.24	4.23	
5.41	'030911E1 (2)'	84.61	3.41		8.69	'030911E1 (26)'	68.22	2.46		9.35	'030911F1 (38)'	66.86	7.95	
	'030911E1 (8)'	97.91	4.80			'030911E1 (32)'	73.52	3.76			'030911F1 (44)'	64.20	10.31	
SNR stdev	'030911E1 (14)'	97.56	2.65		**SNR stdev**	'030911F1 (20)'	68.60	11.22		**SNR stdev**	'030911F1 (50)'	63.92	10.75	
2.67	'030911F1 (2)'	66.54	8.61		4.74	'030911F1 (26)'	64.29	13.89		6.30	'030911A3 (38)'	66.51	12.09	
	'030911F1 (8)'	68.88	9.70			'030911F1 (32)'	62.03	9.25			'030911A3 (44)'	85.18	20.71	
	'030911F1 (14)'	65.21	9.70			'030911A3 (20)'	74.49	10.52			'030911A3 (50)'	82.36	14.86	
	'030911A3 (2)'	80.31	7.13			'030911A3 (26)'	69.25	5.26						
	'030911A3 (8)'	82.04	4.36			'030911A3 (32)'	76.11	16.32						
	'030911A3 (14)'	81.72	4.25											
ACCEL front air	'020211A1 (20)'	71.28	2.15		**ACCEL front water**	'020211A1 (68)'	61.67	0.53		**ACCEL front flow**	'020211A1 (104)'	61.55	1.85	
	'020211A1 (26)'	56.46	1.18			'020211A1 (74)'	59.43	0.83			'020211A1 (110)'	98.57	1.01	
SNR mean	'020211A1 (32)'	63.90	2.14		**SNR mean**	'020211A1 (80)'	60.93	3.22		**SNR mean**	'020211A1 (116)'	97.99	0.57	
1.86	'020411B1 (2)'	87.76	0.06		1.23	'020411B1 (41)'	67.21	0.64		1.36	'020411B1 (80)'	64.00	0.93	
	'020411B1 (8)'	73.60	2.89			'020411B1 (47)'	98.45	1.22			'020411B1 (86)'	Invalid (107.41)'	1.65	x
SNR stdev	'020411B1 (14)'	55.69	0.64		**SNR stdev**	'020411B1 (53)'	82.65	1.24		**SNR stdev**	'020411B1 (92)'	58.87	2.73	
1.43	'020411C1 (2)'	78.68	6.48		1.00	'020411C1 (47)'	89.14	0.98		0.85	'020411C1 (86)'	91.36	0.06	
	'020411C1 (8)'	78.40	2.24			'020411C1 (53)'	60.10	0.17			'020411C1 (92)'	71.53	1.04	
	'020411C1 (14)'	78.93	2.35			'020411C1 (59)'	72.43	1.26			'020411C1 (98)'	92.79	1.31	
	'030211D1 (2)'	59.27	0.72			'030211D1 (29)'	Invalid (102.44)'	1.06	x		'030211D1 (56)'	'Invalid (103.94)'	1.94	x
	'030211D1 (8)'	77.18	2.17			'030211D1 (35)'	74.57	1.04			'030211D1 (62)'	67.17	0.90	
	'030211D1 (14)'	89.97	2.33			'030211D1 (41)'	64.35	1.92			'030211D1 (68)'	88.24	-0.12	x
	'030211C2 (2)'	93.74	1.51			'030211C2 (29)'	87.85	3.76			'030211C2 (56)'	86.89	0.81	
	'030211C2 (8)'	92.65	1.35			'030211C2 (35)'	56.09	1.79			'030211C2 (62)'	58.65	1.89	
	'030211C2 (14)'	83.89	2.46			'030211C2 (41)'	64.03	1.29			'030211C2 (68)'	Invalid (106.85)'	1.84	x
	'030211A2 (2)'	60.30	0.57			'030211A2 (29)'	66.11	0.22			'030211A2 (56)'	Invalid (53.29)'	-2.69	x
	'030211A2 (8)'	97.10	0.30			'030211A2 (35)'	79.76	0.67			'030211A2 (62)'	61.74	1.50	
	'030211A2 (14)'	60.31	1.97			'030211A2 (41)'	69.99	0.12			'030211A2 (68)'	85.66	3.08	
HYDRO front air	'020211A1 (38)'	62.09	1.06		**HYDRO front water**	'020211A1 (86)'	57.73	0.55		**HYDRO front flow**	'020211A1 (122)'	66.89	0.40	
	'020211A1 (44)'	57.90	1.45			'020211A1 (92)'	64.35	-0.53	x		'020211A1 (128)'	95.35	1.55	
SNR mean	'020211A1 (50)'	64.68	1.68		**SNR mean**	'020211A1 (98)'	85.73	1.01		**SNR mean**	'020211A1 (134)'	75.22	2.33	
1.56	'020411B1 (20)'	74.26	2.90		1.66	'020411B1 (59)'	83.11	1.56		1.78	'020411B1 (98)'	70.71	2.55	
	'020411B1 (26)'	68.33	1.13			'020411B1 (65)'	72.59	1.54			'020411B1 (104)'	72.74	4.29	
SNR stdev	'020411B1 (32)'	87.93	1.75		**SNR stdev**	'020411B1 (71)'	67.32	0.80		**SNR stdev**	'020411B1 (110)'	81.38	2.26	
0.83	'020411C1 (20)'	89.53	2.80		1.07	'020411C1 (65)'	57.37	2.71		1.23	'020411C1 (104)'	57.44	0.39	
	'020411C1 (26)'	91.88	0.80			'020411C1 (71)'	Invalid (54.00)'	-0.58	x		'020411C1 (110)'	80.55	0.98	
	'020411C1 (32)'	Invalid (103.67)'	1.69	x		'020411C1 (77)'	90.50	3.50			'020411C1 (116)'	73.41	1.24	
	'020411C1 (38)'	78.65	0.51											

Table A.5: Data for inhale-hold recordings from the dorsal side.

INHALE	Name	HR	SNR			Name	HR	SNR			Name	HR	SNR	
ES back air	'020211A1 (5)'	95.52	0.57		**ES back water**	'020211A1 (59)'	77.71	1.44		**ES back flow**	'030911E1 (41)'	80.90	0.93	
	'020211A1 (11)'	86.04	4.09			'020211A1 (65)'	61.10	1.43			'030911E1 (47)'	85.25	0.38	
SNR mean	'020211A1 (17)'	82.05	4.01		**SNR mean**	'030911E1 (23)'	93.21	1.08		**SNR mean**	'030911E1 (53)'	97.04	1.73	
1.56	'030911E1 (5)'	94.93	11.38	x	1.85	'030911E1 (29)'	75.02	0.65		3.43	'030911F1 (41)'	Invalid (102.36)'	0.20	x
	'030911E1 (11)'	87.77	0.35			'030911E1 (35)'	78.55	1.16	x		'030911F1 (47)'	95.89	1.71	
SNR stdev	'030911E1 (17)'	65.32	0.53		**SNR stdev**	'030911F1 (23)'	67.46	2.57		**SNR stdev**	'030911F1 (53)'	97.44	10.53	
1.38	'030911F1 (5)'	98.53	0.95		1.09	'030911F1 (29)'	68.91	1.17		3.25	'030911A3 (41)'	77.79	3.67	
	'030911F1 (11)'	60.65	0.93			'030911F1 (35)'	74.50	-0.87	x		'030911A3 (47)'	75.41	3.72	
	'030911F1 (17)'	81.31	1.67			'030911A3 (23)'	75.65	2.97			'030911A3 (53)'	85.91	4.81	
	'030911A3 (5)'	56.28	1.47			'030911A3 (29)'	71.80	1.33						
	'030911A3 (11)'	64.97	9.43	x		'030911A3 (35)'	89.52	4.01						
	'030911A3 (17)'	92.14	1.02											
ACCEL back air	'020211A1 (23)'	76.32	9.77	x	**ACCEL back water**	'020211A1 (71)'	82.62	2.23		**ACCEL back flow**	'020211A1 (107)'	86.48	1.11	
	'020211A1 (29)'	94.62	1.17			'020211A1 (77)'	56.49	5.75			'020211A1 (113)'	66.64	1.83	
SNR mean	'020211A1 (35)'	55.11	1.63		**SNR mean**	'020211A1 (83)'	80.06	3.22		**SNR mean**	'020211A1 (119)'	58.62	-0.83	x
1.78	'020411B1 (5)'	75.61	4.83		1.96	'020411B1 (44)'	69.83	0.35		1.37	'020411B1 (83)'	65.73	1.08	
	'020411B1 (11)'	82.70	2.70			'020411B1 (50)'	70.57	3.45			'020411B1 (89)'	77.20	1.91	
SNR stdev	'020411B1 (17)'	71.82	1.22		**SNR stdev**	'020411B1 (56)'	96.34	1.87		**SNR stdev**	'020411B1 (95)'	95.80	2.33	
1.11	'020411C1 (5)'	91.49	0.66		1.35	'020411C1 (50)'	93.68	1.98		0.84	'020411C1 (89)'	Invalid (53.74)'	2.03	x
	'020411C1 (11)'	78.28	1.92			'020411C1 (56)'	84.61	1.05			'020411C1 (95)'	70.67	2.72	
	'020411C1 (17)'	98.15	1.35			'020411C1 (62)'	75.81	-3.34	x		'020411C1 (101)'	65.06	-0.20	x
	'030211D1 (5)'	Invalid (102.62)'	3.31	x		'030211D1 (32)'	69.78	1.35			'030211D1 (59)'	66.93	1.52	
	'030211D1 (11)'	70.59	1.15			'030211D1 (38)'	59.33	1.53			'030211D1 (65)'	91.02	0.29	
	'030211D1 (17)'	Invalid (53.47)'	4.29	x		'030211D1 (44)'	56.26	1.38			'030211D1 (71)'	90.14	0.81	
	'030211C2 (5)'	57.77	3.20			'030211C2 (32)'	74.41	0.84			'030211C2 (59)'	76.32	0.49	
	'030211C2 (11)'	63.94	1.87			'030211C2 (38)'	75.73	1.31			'030211C2 (65)'	86.04	0.35	
	'030211C2 (17)'	91.98	0.62			'030211C2 (44)'	99.11	1.53			'030211C2 (71)'	80.53	0.42	
	'030211A2 (5)'	59.74	0.76			'030211A2 (32)'	60.41	1.64			'030211A2 (59)'	79.10	2.43	
	'030211A2 (11)'	92.92	2.17			'030211A2 (38)'	84.37	0.41			'030211A2 (65)'	96.27	1.91	
	'030211A2 (17)'	62.83	1.47			'030211A2 (44)'	63.05	3.48			'030211A2 (71)'	Invalid (104.01)'	1.36	x
HYDRO back air	'020211A1 (41)'	67.21	0.96		**HYDRO back water**	'020211A1 (89)'	77.99	0.85		**HYDRO back flow**	'020211A1 (125)'	80.71	1.56	
	'020211A1 (47)'	79.71	2.63			'020211A1 (95)'	94.70	1.60			'020211A1 (131)'	57.43	2.04	
SNR mean	'020211A1 (53)'	67.35	1.44		**SNR mean**	'020211A1 (101)'	59.78	0.08		**SNR mean**	'020211A1 (137)'	99.30	2.46	
1.38	'020411B1 (23)'	90.16	0.89		1.53	'020411B1 (62)'	60.74	3.25		1.72	'020411B1 (101)'	58.57	3.01	
	'020411B1 (29)'	95.30	2.21			'020411B1 (68)'	76.29	0.67			'020411B1 (107)'	75.62	1.11	
SNR stdev	'020411B1 (35)'	64.60	0.60		**SNR stdev**	'020411B1 (74)'	84.59	1.83		**SNR stdev**	'020411B1 (113)'	58.66	2.59	
0.70	'020411C1 (23)'	78.31	0.82		1.29	'020411C1 (68)'	94.61	3.92		0.84	'020411C1 (107)'	83.52	1.14	
	'020411C1 (29)'	67.22	1.21			'020411C1 (74)'	86.76	1.15			'020411C1 (113)'	76.30	0.56	
	'020411C1 (35)'	99.70	2.13			'020411C1 (80)'	95.76	0.46			'020411C1 (119)'	94.74	1.05	
	'020411C1 (41)'	84.68	0.88											

Table A.6: Data for inhale-hold recordings for the sensor package.

INHALE		HR		SNR			
	Name	accelometer	hydrophone	accelometer	hydrophone	ac	hy
HYDRO/ACCEL	'020411B1 (38)'	70.62	84.444	1.18	1.11		
inhale hold	'020411C1 (44)'	74.32	62.96	1.11	0.35		
air	'030211D1 (20)'	86.44	88.32	1.49	1.60		
	'030211D1 (23)'	77.00	71.29	1.10	1.33		
	'030211D1 (26)'	78.68	82.96	0.51	1.87		
	'030211C2 (20)'	72.41	91.89	6.55	-0.03		x
	'030211C2 (23)'	87.83	77.57	1.21	1.57		
	'030211C2 (26)'	58.97	Invalid (54.56)'	1.90	0.89		x
	'030211A2 (20)'	Invalid (102.70)'	87.60	1.81	3.15	x	
	'030211A2 (23)'	99.08	68.93	1.55	0.71		
	'030211A2 (26)'	96.80	64.41	1.44	0.95		
			mean	1.80	1.40		
			stdev	1.71	0.81		
HYDRO/ACCEL	'020411B1 (77)'	60.79	59.87	-0.05	0.89	x	
inhale hold	'020411C1 (83)'	70.63	57.53	0.38	1.41		
still water	'030211D1 (47)'	67.20	98.31	1.39	1.13		
	'030211D1 (50)'	60.66	Invalid (108.95)'	0.97	4.60		x
	'030211D1 (53)'	61.57	62.38	2.49	0.55		
	'030211C2 (47)'	96.01	94.04	1.88	0.42		
	'030211C2 (50)'	62.92	89.12	2.96	1.49		
	'030211C2 (53)'	67.22	80.67	1.54	2.65		
	'030211A2 (47)'	Invalid (54.47)'	Invalid (54.01)'	1.07	1.65	x	x
	'030211A2 (50)'	89.03	81.15	0.58	1.42		
	'030211A2 (53)'	58.35	75.81	2.61	1.28		
			mean	1.64	1.25		
			stdev	0.91	0.65		
HYDRO/ACCEL	'020411B1 (116)'	69.20	81.34	0.93	1.18		
inhale hold	'020411C1 (122)'	64.30	97.92	1.06	0.27		
flowing water	'030211D1 (74)'	58.57	63.48	-0.02	0.90	x	
	'030211D1 (77)'	62.85	60.10	5.12	1.53	x	x
	'030211D1 (80)'	83.329	61.64	3.59	0.87	x	x
	'030211C2 (74)'	71.85	79.15	2.34	1.82		
	'030211C2 (77)'	77.81	97.06	1.76	1.50		
	'030211C2 (80)'	96.96	87.78	1.06	1.06		
	'030211A2 (74)'	97.20	86.06	0.73	1.69		
	'030211A2 (77)'	60.32	58.45	1.65	1.14		
	'030211A2 (80)'	84.84	71.82	1.44	0.82		
			mean	1.37	1.15		
			stdev	0.53	0.48		

APPENDIX B

DATA FROM SENSOR COMPARISON EXPERIMENT, V.2

Table B.1: Data for breathing recordings from the ventral side.

BREATHE	Name	SNR	del	add	BPf		Name	SNR	del	add	BPf		Name	SNR	del	add	BPf
ES front air	052512G1 (1)	24.48	0	0	39-55	**ES front water**	052512G1 (37)	12.79	1	1	29-42	**ES front flow**	052512G1 (73)	31.91	1	1	37-49
SNR mean	052512G1 (7)	18.98	0	0	41-56	**SNR mean**	052512G1 (43)	29.16	0	0	29-44	**SNR mean**	052512G1 (79)	30.53	0	0	37-48
22.46	052512H1 (1)	23.25	0	0	32-45	20.63	061312I1 (37)	18.90	0	0	44-56	22.07	061312I1 (73)	12.58	3	2	30-47
SNR stdev	052512H1 (7)	14.85	0	0	34-46	**SNR stdev**	061312I1 (43)	21.67	0	0	48-59	**SNR stdev**	061312I1 (79)	13.24	0	0	45-59
4.74	061312I1 (1)	25.31	0	3	33-49	6.79						10.59					
	061312I1 (7)	27.91	0	0	33-45												
ACCEL front air	052512G1 (13)	26.48	0	0	29-47	**ACCEL front water**	052512G1 (49)	14.88	0	1	26-40	**ACCEL front flow**	052512G1 (85)	14.73	2	2	28-46
SNR mean	052512G1 (19)	23.04	0	0	31-49	**SNR mean**	052512G1 (55)	27.20	0	0	25-37	**SNR mean**	052512G1 (91)	19.47	0	0	36-49
20.18	052512H1 (13)	11.93	0	0	24-40	21.67	052512H1 (37)	10.39	4	7	26-44	10.72	052512H1 (61)	8.56	6	9	22-40
SNR stdev	052512H1 (19)	20.16	0	0	24-38	**SNR stdev**	052512H1 (43)	11.92	1	1	25-39	**SNR stdev**	052512H1 (67)	2.19	11	9	15-35
4.83	061312I1 (13)	19.92	0	0	24-35	10.75	061312I1 (49)	28.90	0	8	24-33	6.35	061312I1 (85)	5.83	5	9	23-48
	061312I1 (19)	19.53	0	0	26-40		061312I1 (55)	36.73	0	14	22-31		061312I1 (91)	13.55	6	6	22-41
PVDF front air	052512G1 (25)	16.96	1	0	75-86	**PVDF front water**	052512G1 (61)	20.85	0	3	36-48	**PVDF front flow**	052512G1 (97)	17.41	2	5	32-50
SNR mean	052512G1 (31)	17.72	0	6	71-79	**SNR mean**	052512G1 (67)	37.54	0	5	34-49	**SNR mean**	052512G1 (103)	19.48	1	9	29-42
18.55	052512H1 (25)	7.46	2	4	70-81	19.94	052512H1 (49)	13.01	3	11	77-89	16.50	052512H1 (73)	15.94	2	2	40-51
SNR stdev	052512H1 (31)	22.19	0	3	33-42	**SNR stdev**	052512H1 (55)	12.11	5	7	68-82	**SNR stdev**	052512H1 (79)	21.89	1	9	26-40
6.52	061312I1 (25)	26.97	0	0	39-49	9.33	061312I1 (61)	16.00	0	0	57-66	4.01	061312I1 (97)	10.85	2	17	28-46
	061312I1 (31)	19.98	0	2	37-50		061312I1 (67)	20.13	0	1	52-62		061312I1 (103)	13.44	9	9	31-47

Table B.2: Data for inhale-hold recordings from the ventral side.

INHALE	Name	SNR	del	add	BPf		Name	SNR	del	add	BPf		Name	SNR	del	add	BPf
ES front air	052512G1 (2)	29.61	0	15	33-48	**ES front water**	052512G1 (38)	10.85	3	3	32-46	**ES front flow**	052512G1 (74)	21.73	3	3	32-44
SNR mean	052512G1 (8)	18.79	0	4	36-47	**SNR mean**	052512G1 (44)	17.89	2	3	30-46	**SNR mean**	052512G1 (80)	17.14	2	8	33-45
22.82	052512H1 (2)	19.46	0	0	31-39	17.15	061312I1 (38)	18.19	0	0	35-50	13.66	061312I1 (74)	4.59	4	10	26-41
SNR stdev	052512H1 (8)	17.35	0	0	31-42	**SNR stdev**	061312I1 (44)	21.68	0	7	27-40	**SNR stdev**	061312I1 (80)	11.19	3	7	30-46
6.32	061312I1 (2)	32.09	0	2	33-52	4.54						7.43					
	061312I1 (8)	19.62	0	0	34-43												
ACCEL front air	052512G1 (14)	25.27	0	12	31-47	**ACCEL front water**	052512G1 (50)	11.32	3	2	24-35	**ACCEL front flow**	052512G1 (86)	10.47	6	8	32-47
SNR mean	052512G1 (20)	12.48	1	12	28-42	**SNR mean**	052512G1 (56)	16.72	0	1	25-36	**SNR mean**	052512G1 (92)	13.12	3	4	30-46
21.51	052512H1 (14)	22.50	0	0	26-38	17.15	052512H1 (38)	15.99	2	2	35-57	20.40	052512H1 (62)	34.10	1	2	34-44
SNR stdev	052512H1 (20)	21.95	0	6	32-44	**SNR stdev**	052512H1 (44)	14.34	3	5	21-35	**SNR stdev**	052512H1 (68)	14.78	2	2	21-34
4.65	061312I1 (14)	24.78	0	0	35-45	4.38	061312I1 (50)	22.39	0	2	22-32	10.03	061312I1 (86)	18.29	2	3	24-36
	061312I1 (20)	22.09	0	0	37-47		061312I1 (56)	22.14	1	3	22-33		061312I1 (92)	31.68	0	16	24-33
PVDF front air	052512G1 (26)	29.33	0	15	71-79	**PVDF front water**	052512G1 (62)	22.35	2	3	29-45	**PVDF front flow**	052512G1 (98)	24.69	1	11	23-31
SNR mean	052512G1 (32)	20.82	3	16	38-48	**SNR mean**	052512G1 (68)	17.93	1	2	29-40	**SNR mean**	052512G1 (104)	8.70	1	10	26-41
27.31	052512H1 (26)	33.26	2	12	37-47	15.84	052512H1 (50)	12.94	2	5	39-51	16.25	052512H1 (74)	18.36	2	10	38-51
SNR stdev	052512H1 (32)	24.27	0	9	31-45	**SNR stdev**	052512H1 (56)	15.85	2	4	37-51	**SNR stdev**	052512H1 (80)	12.02	0	0	18-33
6.81	061312I1 (26)	19.73	0	0	39-50	4.06	061312I1 (62)	15.34	0	0	26-34	5.61	061312I1 (98)	18.61	1	1	32-50
	061312I1 (32)	36.45	0	12	43-55		061312I1 (68)	10.63	1	1	28-50		061312I1 (104)	15.11	3	14	29-50

Table B.3: Data for exhale-hold recordings from the ventral side.

EXHALE	Name	SNR	del	add	BPf			Name	SNR	del	add	BPf			Name	SNR	del	add	BPf
ES front air	052512G1 (3)	21.92	0	3	37-45		**ES front water**	052512G1 (39)	19.72	2	3	28-45		**ES front flow**	052512G1 (75)	31.59	0	1	32-47
SNR mean	052512G1 (9)	22.59	0	2	39-52		**SNR mean**	052512G1 (45)	23.56	0	0	27-45		**SNR mean**	052512G1 (81)	18.96	0	0	27-41
21.94	052512H1 (3)	20.53	0	0	39-58		22.03	061312I1 (39)	24.50	0	0	38-55		26.85	061312I1 (75)	27.91	0	14	25-40
SNR stdev	052512H1 (9)	18.25	0	0	31-43		**SNR stdev**	061312I1 (45)	20.33	0	0	53-64		**SNR stdev**	061312I1 (81)	28.96	0	13	32-52
3.37	061312I1 (3)	20.25	0	16	37-49		2.36							5.49					
	061312I1 (9)	28.09	0	16	38-49														
ACCEL front air	052512G1 (15)	21.94	0	0	31-44		**ACCEL front water**	052512G1 (51)	25.74	0	0	25-40		**ACCEL front flow**	052512G1 (87)	14.98	0	0	30-42
SNR mean	052512G1 (21)	37.00	0	4	41-54		**SNR mean**	052512G1 (57)	26.12	0	0	30-39		**SNR mean**	052512G1 (93)	19.87	1	1	22-31
23.67	052512H1 (15)	18.36	0	0	20-32		20.48	052512H1 (39)	11.16	0	0	40-55		13.85	052512H1 (63)	17.08	1	2	33-46
SNR stdev	052512H1 (21)	23.30	1	2	25-38		**SNR stdev**	052512H1 (45)	14.36	1	0	24-40		**SNR stdev**	052512H1 (69)	3.59	7	12	16-37
6.74	061312I1 (15)	20.36	0	1	29-42		6.24	061312I1 (51)	22.09	1	6	19-27		6.48	061312I1 (87)	19.10	6	6	26-50
	061312I1 (21)	21.05	3	6	29-42			061312I1 (57)	23.43	0	0	23-36			061312I1 (93)	8.47	3	10	21-35
PVDF front air	052512G1 (27)	24.45	0	0	62-78		**PVDF front water**	052512G1 (63)	21.84	0	0	36-56		**PVDF front flow**	052512G1 (99)	21.90	1	2	40-50
SNR mean	052512G1 (33)	34.64	1	6	64-82		**SNR mean**	052512G1 (69)	24.45	0	0	30-47		**SNR mean**	052512G1 (105)	29.97	0	12	28-41
20.59	052512H1 (27)	14.89	0	0	70-82		19.38	052512H1 (51)	12.63	6	9	72-84		22.92	052512H1 (75)	13.89	1	1	66-78
SNR stdev	052512H1 (33)	15.14	1	0	71-85		**SNR stdev**	052512H1 (57)	15.91	1	1	73-86		**SNR stdev**	052512H1 (81)	13.99	5	7	70-78
8.64	061312I1 (27)	23.37	1	8	31-48		4.49	061312I1 (63)	18.76	3	5	39-56		7.55	061312I1 (99)	27.89	1	7	32-46
	061312I1 (33)	11.04	1	6	40-54			061312I1 (69)	22.70	1	8	37-54			061312I1 (105)	29.88	1	12	35-49

Table B.4: Data for all recordings from the dorsal side.

BREATHE	Name	SNR	del	add	BPf		INHALE	Name	SNR	del	add	BPf		EXHALE	Name	SNR	del	add	BPf
ES back air	061312I1 (4)	15.96	2	22	34-47		**ES back air**							**ES back air**	052512H1 (6)	12.74	3	10	31-44
SNR mean	061312I1 (10)	29.01	0	14	33-42		**SNR mean**							**SNR mean**	061312I1 (6)	20.28	1	22	28-41
22.48							N/A							19.15	061312I1 (12)	24.42	4	5	34-47
SNR stdev							**SNR stdev**							**SNR stdev**					
9.23							N/A							5.92					
ACCEL back air	061312I1 (22)	11.81	2	11	21-35		**ACCEL back air**	052512H1 (17)	36.35	0	11	49-60		**ACCEL back air**	052512H1 (18)	14.90	3	11	27-38
SNR mean							**SNR mean**							**SNR mean**	052512H1 (24)	29.89	3	13	13-21
11.81							36.35							17.20	061312I1 (24)	11.62	2	16	27-45
SNR stdev							**SNR stdev**							**SNR stdev**	061312I1 (60)	12.38	3	17	30-48
N/A							N/A							8.58					
PVDF back air	061312I1 (28)	8.17	5	18	20-33		**PVDF back air**							**PVDF back air**	052512G1 (30)	28.23	1	16	38-46
SNR mean	061312I1 (34)	7.20	6	16	24-40		**SNR mean**							**SNR mean**	061312I1 (30)	20.15	4	12	39-50
7.68							N/A							20.83	061312I1 (36)	14.10	2	7	32-41
SNR stdev							**SNR stdev**							**SNR stdev**					
0.69							N/A							7.09					

REFERENCES

Berntson, G. and S. Boysen (1984). "Cardiac startle and orienting responses in the great apes." Behavioral neuroscience **98**(5): 914-918.

Burgess, W. C., P. L. Tyack, et al. (1998). "A programmable acoustic recording tag and first results from free-ranging northern elephant seals." Deep-Sea Research Part II **45**(7): 1327-1351.

CIMRS Bioacoustics Lab (2010, 2010). "Ishmael." Retrieved January 10, 2013, from http://www.bioacoustics.us/ishmael.html.

Claireaux, G., D. Webber, et al. (1995). "Physiology and behaviour of free-swimming Atlantic cod (Gadus morhua) facing fluctuating temperature conditions." Journal of experimental biology **198**(1): 49-60.

Cox, T. M., T. J. Ragen, et al. (2006). "Understanding the impacts of anthropogenic sound on beaked whales." Journal of Cetacean Research and Management **7**(3): 177-187.

Elsner, R. (1966). "Diving Bradycardia in the Unrestrained Hippopotamus." Nature **212**: 408.

Elsner, R., D. W. Kenney, et al. (1966). "Diving Bradycardia in the Trained Dolphin." Nature **212**: 407-408.

Fletcher, S., B. J. Le Boeuf, et al. (1996). "Onboard acoustic recording from diving northern elephant seals." The Journal of the Acoustical Society of America **100**(4 Pt 1): 2531-2539.

Graham, F. K. (1979). "Distinguishing among orienting, defense, and startle reflexes." The orienting reflex in humans: 137-167.

Guillot, F. M. and D. Trivett (2003). "A dynamic Young's modulus measurement system for highly compliant polymers." The Journal of the Acoustical Society of America **114**: 1334-1345.

Johnson, M. (2001, September 28, 2011). "OLI Grant: Sensors for Velocity and Heart Rate Acquisition on Wild Marine Mammals ". Retrieved October 27, 2011, from http://www.whoi.edu/page.do?pid=10517&tid=282&cid=2684.

Johnson, M. P. and P. L. Tyack (2003). "A digital acoustic recording tag for measuring the response of wild marine mammals to sound." IEEE Journal of Oceanic Engineering **28**(1): 3-12.

Kasoev, S. G. (2005). "Heart sounds as a result of acoustic dipole radiation of heart valves." Acoustical Physics **51**(6): 680-687.

King, R. L., J. L. Jenks Jr, et al. (1953). "The electrocardiogram of a beluga whale." Circulation **8**(3): 387-393.

Kinsler, L. E., A. R. Frey, et al. (1999). "Fundamentals of acoustics." Fundamentals of Acoustics, 4th Edition, by Lawrence E. Kinsler, Austin R. Frey, Alan B. Coppens, James V. Sanders, pp. 560. ISBN 0-471-84789-5. Wiley-VCH, December 1999. **1**.

Ko, S. H. and H. H. Schloemer (1992). "Flow noise reduction techniques for a planar array of hydrophones." The Journal of the Acoustical Society of America **92**: 3409.

Levine, H. and J. Schwinger (1948). "On the radiation of sound from an unflanged circular pipe." Physical review **73**(4): 383-406.

Lippincott (2009). Auscultation Skills: Breath and Heart Sounds, Lippincott Williams & Wilkins.

MacArthur, R. A., R. H. Johnston, et al. (1979). "Factors influencing heart rate in free-ranging bighorn sheep: a physiological approach to the study of wildlife harassment." Canadian Journal of Zoology **57**(10): 2010-2021.

Madigosky, W. M. and G. F. Lee (1979). "Automated dynamic Young's modulus and loss factor measurements." The Journal of the Acoustical Society of America **66**: 345-349.

Madsen, P. T., M. Johnson, et al. (2005). "Biosonar performance of foraging beaked whales (Mesoplodon densirostris)." Journal of experimental biology **208**(2): 181-194.

Meijler, F. L., F. H. M. Wittkampf, et al. (1992). "Electrocardiogram of the humpback whale (Megaptera noaeangliae) with specific reference to atrioventricular transmission and ventricular excitation." Journal of the American College of Cardiology **20**(2): 475-479.

Meir, J. U., T. K. Stockard, et al. (2008). "Heart rate regulation and extreme bradycardia in diving emperor penguins." Journal of experimental biology **211**(8): 1169-1179.

Miksis, J. L., M. D. Grund, et al. (2001). "Cardiac response to acoustic playback experiments in the captive bottlenose dolphin (Tursiops truncatus)." Journal of Comparative Psychology **115**(3): 227-232.

Nowacek, D. P., M. P. Johnson, et al. (2004). "North Atlantic right whales (Eubalaena glacialis) ignore ships but respond to alerting stimuli." Proceedings of the Royal Society of London. Series B: Biological Sciences **271**(1536): 227-231.

Organisation Cetacea. "The Beaked Whale Resource." Retrieved January 10, 2013, from http://www.beakedwhaleresource.com/quicklinks.htm.

Pierce, A. D. (1989). Acoustics: An Introduction to Its Physical Principles and Applications, Acoustical Soc. of America (American Inst. of Physics).

Ponganis, P. J. and G. L. Kooyman (1999). "Heart rate and electrocardiogram characteristics of a young California gray whale (Eschrichtius robustus)." Marine mammal science **15**(4): 1198-1207.

Ridgway, S. H. and R. Howard (1979). "Dolphin lung collapse and intramuscular circulation during free diving: evidence from nitrogen washout." Science **206**(4423): 1182-1183.

Ronan Jr, J. A. (1992). "Cardiac auscultation: the first and second heart sounds." Heart disease and stroke: a journal for primary care physicians **1**(3): 113-116.

Spencer, M. P., T. A. Gornall, et al. (1967). "Respiratory and cardiac activity of killer whales." Journal of Applied Physiology **22**(5): 974-981.

Tyack, P. L., M. Johnson, et al. (2006). "Extreme diving of beaked whales." Journal of experimental biology **209**(21): 4238-4253.

Williams, T. M., W. A. Friedl, et al. (1993). "The physiology of bottlenose dolphins (Tursiops truncatus): heart rate, metabolic rate and plasma lactate concentration during exercise." Journal of experimental biology **179**(1): 31-46.

Williams, T. M., J. E. Haun, et al. (1999). "The diving physiology of bottlenose dolphins (Tursiops truncatus). I. Balancing the demands of exercise for energy conservation at depth." Journal of experimental biology **202**(20): 2739-2748.

Williams, T. M., D. Noren, et al. (1999). "The diving physiology of bottlenose dolphins (Tursiops truncatus). III. Thermoregulation at depth." Journal of experimental biology **202**(20): 2763-2769.

Wolf, S. (1965). "The bradycardia of the dive reflex—a possible mechanism of sudden death." Transactions of the American Clinical and Climatological Association **76**: 192-200.

Yoganathan, A. P., R. Gupta, et al. (1976). "Use of the fast Fourier transform in the frequency analysis of the second heart sound in normal man." Medical and Biological Engineering and computing **14**(4): 455-460.

Yoganathan, A. P., R. Gupta, et al. (1976). "Use of the fast Fourier transform for frequency analysis of the first heart sound in normal man." Medical and Biological Engineering and computing **14**(1): 69-73.

Zavarehei, E. (2005). Wiener Filter. MATLAB Central File Exchange.